Mechanism of Adenylate Kinase. Is There a Relationship between Local Substrate Dynamics, Local Binding Energy, and the Catalytic Mechanism?†

Charles R. Sanders II,‡ Gaochao Tian,§ and Ming-Daw Tsai*
Department of Chemistry, The Ohio State University, Columbus, Ohio 43210
Received October 18, 1988; Revised Manuscript Received June 28, 1989

ABSTRACT: Adenylyl (β,γ-methylene)diphosphonic acid (AMPPCP) labeled with deuterium at the adenine ring ([8-^{2}H]AMPPCP) and at the β,γ-methylene group (AMPPCD$_2$P), as well as adenosine 5'-monophosphate labeled at the adenine ring ([8-^{2}H]AMP), was synthesized and used for deuterium nuclear magnetic resonance (NMR) determination of effective correlation times (τ_c) of the free nucleotide and the complexes with adenylate kinase (AK). Extensive and rigorous control experiments and theoretical analysis were performed to justify the validity of the experimental approaches, particularly the fast exchange condition, and the reliability of the τ_c values obtained. For the free nucleotide, the results suggest that the phosphonate group of free AMPPCP possesses appreciable local mobility relative to the adenine ring and that complexation with Mg^{2+} greatly reduced such a local mobility. For the complexes with AK, effective τ_c values of 7, 15, 28, 28, and 27 ns were obtained for AMPPCD$_2$P, MgAMPPCD$_2$P, [8-^{2}H]AMPPCP, Mg[8-^{2}H]AMPPCP, and [8-^{2}H]AMP, respectively. These results suggest that the adenine ring of substrates is rigidly bound in all cases, that the phosphonate chain of AMPPCP possesses considerable local mobility, and that Mg^{2+} reduces such local mobility but does not totally immobilize it. The local dynamics of the analogues bound to AK was correlated with local binding energies for the binding of MgAMPPCP and MgATP to AK estimated from the binding studies by proton NMR and other techniques, in conjunction with the binding theory of Jencks [Jencks, W. P. (1981) *Proc. Natl. Acad. Sci. U.S.A. 78*, 4046-4050]. The results suggest that no general correlation exists between the local rigidity of portions of a bound substrate and the corresponding (ground state) local binding energy contributed by these portions. In particular, the adenosine moiety contributes little to the binding energy despite the fact that the adenine ring is rigidly bound; the triphosphate (PPP_i) moiety behaves oppositely; Mg^{2+} immobilizes the triphosphate chain but does not enhance binding. Finally, isomers of the substitution-inert β,γ-bidentate Cr(III) complexes of adenosine 5'-triphosphate (CrATP) were used to probe two unresolved catalytic problems implicitly related to the local mobility of the phosphonate chain of AMPPCP in the AK-MgAMPPCP complex. The first problem concerns the result of electron paramagnetic resonance (EPR) studies that (R_p)- but not (S_p)-[β-^{17}O]ATP caused a line broadening in the Mn(II) EPR spectrum of the AK-MnATP complex [Kalbitzer, H. R., Marquetant, R., Connolly, B. A., & Goody, R. S. (1983) *Eur. J. Biochem. 133*, 221-227]. This would require that AK has already expressed its stereochemical constraint at the ground state and would argue against local mobility of the triphosphate chain in AK-MgATP. We have found that the K_i values for the mixture, the Δ isomer, and the Λ isomer of CrATP are 16, 11, and 20 μM, respectively, which suggest that ground-state binding by AK is stereochemically permissive. This is further supported by the observation that AK allows epimerization and conformational isomerization between isomers of CrATP at the active site, which also suggests that AK should be able to utilize "wrong isomers" of bound MgATP effectively by allowing them to convert to a productive isomer. The results of both problems fully support the conclusion that the phosphonate chain of AK-MgAMPPCP possesses considerable local mobility and illuminate the relationship between the dynamics of bound substrates and the catalytic mechanism.

The relationships between the motional dynamics of substrates, binding energy, and enzymic catalysis are fundamental issues in enzymology but have received relatively little experimental attention due to difficulty in accurate determination of the mobility of substrates bound to the active site of enzymes. In this paper we report the following results related to these issues: (1) The local mobilities of specifically deuterated AMPPCP[1] (see Scheme I), MgAMPPCP, and AMP free in solution and bound to AK were determined from quantitative measurements of deuterium NMR relaxation

† This work was supported by a grant from the National Science Foundation (DMB-8603553). M.-D.T. is a Camille and Henry Dreyfus Teacher-Scholar, 1985-1990. C.R.S. was a Phillips Petroleum Graduate Fellow, 1988. The Bruker AM-500 and MSL-300 NMR spectrometers were partially funded by NIH Grant RR 01458. This is paper 5 in the series "Mechanism of Adenylate Kinase". For paper 4, see Tian et al. (1988). A preliminary account of part of this work has been published (Sanders & Tsai, 1988).

‡ Present address: Department of Chemistry, Yale University, New Haven, CT 06511.

§ Present address: Department of Chemistry, University of California at Berkeley, Berkeley, CA 94720.

[1] Abbreviations: Ado, adenosine; ADP, adenosine 5'-diphosphate; AK, adenylate kinase; AMP, adenosine 5-'monophosphate; AMPPCP, adenylyl (β,γ-methylene)diphosphonic acid; AMPPCD$_2$P, adenylyl (β,γ-dideuteriomethylene)diphosphonic acid; AP$_5$A, P^1,P^5-bis(5'-adenosyl) pentaphosphate; ATP, adenosine 5'-triphosphate; 2'-dATP, 2'-deoxyadenosine 5'-triphosphate; 3'-dATP, 3'-deoxyadenosine 5'-triphosphate; CHES, 2-(cyclohexylamino)ethanesulfonic acid; DTE, dithioerythritol; DTT, dithiothreitol; EDTA, ethylenediaminetetraacetic acid; EPR, electron paramagnetic resonance; FID, free induction decay; Hepes, *N*-(2-hydroxyethyl)piperazine-*N*'-2-ethanesulfonic acid; HPLC, high-pressure liquid chromatography; K_a, association constant; K_d, dissociation constant; MES, 2-(*N*-morpholino)ethanesulfonic acid; NMR, nuclear magnetic resonance; NOE, nuclear Overhauser effect; PEG, poly(ethylene glycol); PEI, poly(ethylene imine); PP_i, pyrophosphate; PPP_i, triphosphate; T_1, longitudinal relaxation time; T_2, transverse relaxational time; T_q, the extreme narrowing quadrupolar relaxation time; TEAB, triethylammonium bicarbonate; TLC, thin-layer chromatography; Tris, 2-amino-2-(hydroxymethyl)-1,3-propanediol; TSP, 3-(trimethylsilyl)-propionic acid; τ_c, correlation time.

0006-2960/89/0428-9028$01.50/0

Scheme I: Structures and Synthesis of $AMPPCD_2P$ and [8-^{2}H]AMPPCP

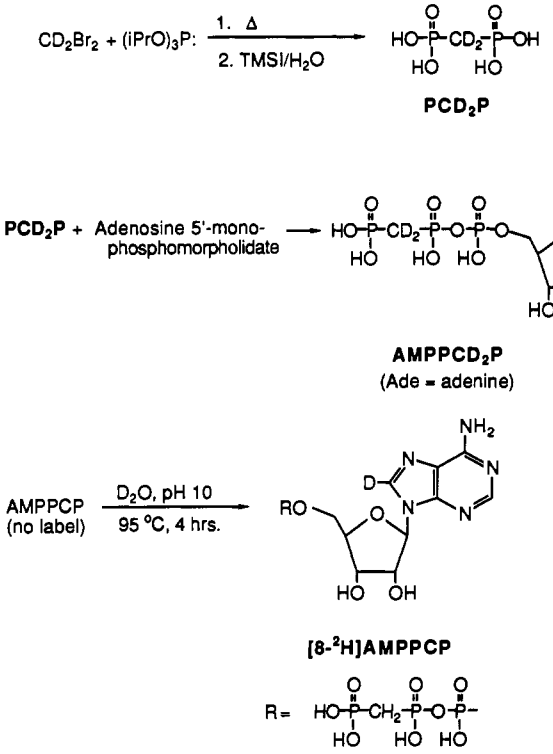

times. The results indicate that the triphosphonate chain of bound AMPPCP has considerable local mobility relative to the adenine ring and that binding of Mg^{2+} reduces some, but not all of, such mobility. (2) The dynamic properties were then correlated with the local binding energies determined from the binding constants of various analogues (partial structures) of ATP and AMPPCP by using proton NMR and other techniques. The results suggest that there is no generalizable relationship between local substrate dynamics and local binding energies. (3) Possible significance of the local mobility of the triphosphonate moiety of bound AMPPCP in catalysis by AK was suggested by the observation that both Δ and Λ isomers of β,γ-bidentate $Cr^{III}(H_2O)_4ATP$ (abbreviated CrATP) can bind to, and can interconvert (epimerize) at, the active site of AK.

Materials and Methods

Theoretical Basis for Local Substrate Dynamics and Local Binding Energy. "Quadrupolar NMR" (NMR of quadrupolar nuclei) is a direct method to determine the dynamics of protein–ligand complexes (Sanders & Tsai, 1989). Deuterium NMR was chosen for the present study because it is possible to determine the relaxation times and effective correlation times τ_c accurately, provided that complication by exchange processes can be dealt with properly as described under Results and Discussion. For deuterium, the physical descriptions of its quadrupolar NMR relaxation rates in the absence of chemical exchange and under effectively isotropic conditions are (Allegrini et al., 1985; Abragam, 1961)

$$1/T_{1q} = (3\pi^2/20)(e^2qQ/h)^2(1 + \eta^2/3) \times \left(\frac{2\tau_c}{1 + \omega^2\tau_c^2} + \frac{8\tau_c}{1 + 4\omega^2\tau_c^2}\right) \quad (1)$$

$$1/T_{2q} = (3\pi^2/20)(e^2qQ/h)^2(1 + \eta^2/3) \times \left(3\tau_c + \frac{5\tau_c}{1 + \omega^2\tau_c^2} + \frac{2\tau_c}{1 + 4\omega^2\tau_c^2}\right) \quad (2)$$

where e^2qQ/h is the quadrupolar coupling constant, ω is the angular larmor frequency, τ_c is the rotational correlation time, and η is the asymmetry parameter. Due to the nonspherical symmetry of the C–D bond, the quadrupolar coupling constants for deuterium are sufficiently high to dictate that quadrupolar relaxation is effectively the only relaxation mechanism, and the assumptions $T_1 = T_{1q}$ and $T_2 = T_{2q}$ are justified. Thus, *τ_c can be calculated directly from the experimentally determined T_1 and/or T_2 if e^2qQ/h and η are known.*

Our approach to determine local binding energies was to determine the binding constants of various analogues (partial structures) of ATP and AMPPCP by using proton NMR and other techniques, which then allowed calculation of the binding energy, $\Delta G°$, of various analogues. It is tempting to suppose that the overall binding constant for a protein and a multisegmental molecule such as ATP will be the sum of the observed binding energies for the individual segments (e.g., adenosine and triphosphate) with the protein. Jencks (1981) warned against this oversimplification and suggests more accurate ways to approach the question of additive contributions to binding. Applying his theory to our system yields

$$\Delta G°_{MgATP} = \Delta G^i_{Ado} + \Delta G^i_{MgPPP_i} + \Delta G^{conn} \quad (3)$$

where ΔG^{conn} is a "connectivity" energy (containing miscellaneous energetic contributions that are due to the connection of Ado and $MgPPP_i$) and ΔG^i are "intrinsic" binding energies. In the present case we prefer to use the term "local" binding energies since intrinsic binding energies have come to be associated with the maximal binding energy that is expressed in the transition state of enzyme–substrate complexes, while our studies deal only with the ground-state complex. Jencks (1981) suggested that local binding energies can be readily estimated from experimentally observed binding energies. For example, again applying his equation to our system yields

$$\Delta G^i_{Ado} = \Delta G°_{MgATP} - \Delta G°_{MgPPP_i} \quad (4)$$

$$\Delta G^i_{MgPPP_i} = \Delta G°_{MgATP} - \Delta G°_{Ado} \quad (5)$$

These and analogous equations have been used to calculate ΔG^i values from the various $\Delta G°$ values determined by proton NMR and other binding studies.

Materials. Chemicals used in the synthesis of $AMPPCD_2P$, D_2O, deuterium-depleted H_2O, $CrCl_3$, 99.999% $MgCl_2·6H_2O$, and the sodium salt of [$^2H_4$]TSP were purchased from Aldrich. All nucleotides and general biochemicals were purchased from Sigma. [2-^{3}H]ATP was obtained from Amersham and perdeuterated Trizma base from MSD Isotopes. Ion-exchange resins were obtained from Pharmacia or Bio-Rad; PEG 20000 was obtained from Fluka, silica gel TLC plates from E. M. Sciences, and puratronic grade $Mg(NO_3)_2·6H_2O$ from Alfa. Scinti-Verse E scintillation cocktail was purchased from Fisher and PEI–cellulose (Machery-Nagel PEI/UV_{254}, 0.1 mm precoated) from Brinkmann; HPLC columns were purchased from Beckman. The AK from chicken muscle[2] (used in all but the epimerization studies) was purified from *Escherichia*

[2] The results of AK from porcine and rabbit muscles (used in many previous studies) and from chicken muscle are often compared directly because the primary structures of these three variants of AK are ≥85% homologous. Complete sequences of all three can be found in Kishi et al. (1986), except that the numbering in Kishi et al. (1986) is shifted by one relative to the commonly used numbering system for AK1 (mammalian muscle AK) (Schulz et al., 1986). For the reasons described in Tian et al. (1988), we use the numbering of Schulz et al. (1986) in our papers.

coli JM103 harboring pKK-cAK1-1 (containing the cloned and overproduced chicken muscle AK gene; Kishi et al., 1986) as described previously (Tian et al., 1988; Tanizawa et al., 1987). The AK from porcine muscle[2] used in the epimerization studies was purified as described previously (Shyy et al., 1987).

Syntheses of [8-^{2}H]AMPPCP, [8-^{2}H]AMP, and AMPPCD$_2$P. The procedures are outlined in Scheme I. AMPPCP was dissolved in D_2O containing 10 mM CHES, the pH (uncorrected) was raised to 10, and the sample was dried by rotary evaporation. The nucleotide was redissolved in D_2O to a concentration of 0.1 g/mL, and the pH (*all pH values reported are not corrected for the deuterium isotope effect*) was then readjusted to ca. 10. This solution was transferred to a 13 × 100 mm test tube that was heated on a heating block for 4 h at 95 °C. The produce was a ca. 1:1 mixture of AMP and AMPPCP with the level of deuteration at the adenine C-8 position being 90% as observed by ^{1}H NMR. [8-^{2}H]AMPPCP was purified by ion-exchange chromatography using DEAE-Sephadex A-25 equilibrated with TEAB. The nucleotides were applied as a basic aqueous solution and eluted with a linear gradient of water to 0.65 M TEAB. Fractions containing the nucleotides were identified by their absorbance at 259 nm and TLC on silica gel, and the AMPPCP was pooled and processed to a K^+ salt by use of the method of Reynolds et al. (1983). The [8-^{2}H]AMPPCP was judged to be pure by ^{1}H NMR and TLC on silica gel. ^{31}P NMR sometimes indicated the presence of two impurities, both 10% or less, which were methylenediphosphonic acid and (probably) inorganic phosphate. The silica gel TLC solvent system used in all experiments was isobutyric acid/concentrated NH_4OH/H_2O (66/1/33) (Pharmacia, 1984). [8-^{2}H]AMP was synthesized by the same method and observed to be totally pure by TLC and ^{1}H and ^{31}P NMR.

For the synthesis of AMPPCD$_2$P, tetraisopropyl [$^2H_2$]-methylenediphosphonate was synthesized (20–40% yield) in a drybox under argon by the method of Roy (1966) using CD_2Br_2 and triisopropyl phosphite that had been distilled and dried with molecular sieves. This ester was observed to be ca. 90% deuterated by fast atom bombardment mass spectroscopy and was converted to [$^2H_2$]methylenediphosphonic acid with no further loss of deuteration (as observed by ^{1}H NMR) by transesterification with trimethylsilyl iodide (Olah & Nurang, 1982) followed by water hydrolysis. The original HCl ester hydrolysis described by Roy (1966) was found to result in H–D exchange. The product was partially purified by ion-exchange methods and converted to its bis(tributylammonium) dipyridinium salt (Myers et al., 1965) and reacted with adenosine phosphomorpholidate in dry pyridine (Moffatt & Khorana, 1961) to produce AMPPCD$_2$P (40–60% yield) which was purified and processed as described for [8-^{2}H]AMPPCP and judged to be pure by silica gel TLC and ^{1}H NMR and >90% pure by ^{31}P NMR (methylenediphosphonic acid was sometimes observed to be present at a low level).

Preparation of Nucleotide Stock Solutions for NMR. For ^{2}H NMR, deuterated AMPPCP or AMP was dissolved in ^{2}H-depleted H_2O, and a few beads of Chelex 100 were added followed by pH adjustment to 7.0. The AMPPCP concentration was determined by measuring absorbance at 259 nm and was stored at −65 °C between NMR experiments. Stock solution concentrations were 50–250 mM. These stock solutions were used both to make 6 mM deuterated nucleotide solutions at pH 7.0 and 10.0 for titration by Mg^{2+} and to titrate AK solutions. The concentration of Mg^{2+} in stock $Mg(NO_3)_2$ solutions used in AMPPCP titrations was determined by volumetric titration with EDTA (Schenk et al., 1977). In pH 10 titrations of AMPPCP by Mg^{2+} the solution was not buffered, and the pH was readjusted to 10 after every second or third addition of $Mg(NO_3)_2$.

For proton NMR, ligand stock solutions (ATP, AMP, etc.) were made by dissolution of the ligand into D_2O, addition of a few grains of dried Chelex, and adjustment of the pH to the appropriate value (7.0 or 8.0). In some instances these solutions were lyophilized followed by redissolution and readjustment (when necessary) of the pH. Nucleoside and nucleotide concentrations were determined by their absorbances at 259 nm, while inorganic ligand concentrations were estimated on the basis of their dry weights. In the case of the ATP used for the MgATP titration of AK, further purification of the ATP was accomplished by using DEAE-Sephadex A-25. Stock solutions of adenosine (>50 mM) had to be warmed on a heating block at 90 °C in small test tubes equipped with a condensor. In this manner solubility was maintained with no change in the concentration occurring and with no adenosine breakdown even over a period of a number of hours, as determined by UV absorbancy, TLC, and proton NMR.

Preparation of AK Samples for NMR. The purified enzyme was originally a 1–2 mg/mL solution in 5 mM imidazole hydrochloride, 1 mM DTT, and 0.1 mM EDTA, pH 6.9. For ^{2}H NMR studies the enzyme was usually transferred to dialysis tubing and concentrated by placing the tubing directly onto dry PEG 20000 or into a buffered PEG syrup to a concentration of >4 mg/mL. A certain amount of low molecular weight PEG was found to enter the dialysis tubing, which was observed in the ^{2}H NMR spectra. This was found to have no effect on ^{2}H NMR results but makes this method of concentration unsuitable for ^{1}H NMR work. Following dialysis the concentration of the enzyme was determined by measuring absorbance at 280 nm and assuming $\epsilon_{280(0.1\%)} = 0.5$. This approximate concentration was designated Y mg/mL, and the enzyme was then dialyzed against $Y/45$ × 10 mM K^+Hepes or imidazole hydrochloride, $Y/45$ × 150 mM KCl, 1 mM mercaptoethanol, and 0.2 mM DTT, pH 7.0, and then lyophilized. At the time of the NMR experiment 90 mg of this preparation was dissolved in 1.91 mL of 40 mM K^+Hepes or imidazole hydrochloride and 0.1 mM EDTA, pH 7.0, in ^{2}H-depleted H_2O. Extra DTT was added at this point and at various times during the NMR epxeriment. Following centrifugation for 10–15 min at 8000*g*, 1.7–1.85 mL of this preparation was placed into a 10-mm NMR tube and was ready for titration. By calculation, the solution contains 1.6 mM AK, 117 mM KCl, 45 mM K^+Hepes or imidazole hydrochloride, 0.1 mM EDTA, and 1–2 mM DTT, pH 7.0. Such solutions were used in all of the ^{2}H NMR studies involving AK described in this paper. The actual AK concentration was determined for calculational purposes by using the coupled assay system and assuming that at 30 °C the enzyme exhibits an apparent specific activity (at 2 mM ATP and AMP) of 1500 units/mg (Tian et al., 1988) and was found to vary from 1 to 1.5 mM.

For proton NMR studies KCl was added to the AK solution (in 5 mM imidazole hydrochloride, 0.1 mM EDTA, 1 mM DTT, pH 6.9) to a concentration of 15–30 mM, and the solution was lyophilized. It was observed that the AK concentration needs to be ≥2 mg/mL for AK to lyophilize without denaturing. The dried enzyme was dissolved to a concentration of 20 mg/mL in 1 mM K^+Hepes, 65 mM KCl, 0.1 mM EDTA, and 1 mM DTT, pH 7.8, and dialyzed against 4 L of this same buffer. Following dialysis exactly 1.2 mL of the enzyme was placed into a 15-mL pear-shaped flask along with

a small number of beads of Chelex 100 followed by lyophilization, redissolution in D_2O, and relyophilization. Immediately before ^1H NMR experiments exactly 1.2 mL of 75 mM perdeuterated Tris-DCl, pH 8.0, in D_2O was added to the dried enzyme, still in the pear-shaped flask, and to this was added DTT to a total concentration of 1.5 mM along with a small amount of [$^2H_4$]TSP as an internal reference. The resulting solution was then passed through a D_2O-rinsed Gelman Acrodisk (No. 4192), and two 0.4–0.5-mL portions of the resulting solution were transferred to two 5-mm NMR tubes. The solution composition was 0.2–0.9 mM AK in 75 mM perdeuterated Tris-DCl, 65 mM KCl, 1.5 mM DTT, 1 mM K^+Hepes, and 0.1 mM EDTA, pH 8.0. The exact AK concentration was determined by measuring integrals of individual AK peaks (C2–H of histidine residues) relative to those arising from ligands added to a known concentration.

Deuterium NMR Methods. ^2H NMR was usually run unlocked on a Bruker MSL-300 spectrometer operating at 46.1 MHz, although some spectra were also obtained at 77.8 MHz on a Bruker AM-500 spectrometer. Shimming to <3-Hz inhomogeneity was routinely achieved by "shimming on the FID" from an aqueous [$^2H_6$]acetone standard. Inhomogeneity could be monitored during the actual titrations by measuring the line width of the HDO peak, which has a natural line width of <1 Hz. Samples containing AK were not spun. From the HDO line width it was observed that in all AK titrations the contributions of field inhomogeneity and field drift were negligible.

Spin–lattice relaxation times (T_1) were determined by the inversion-recovery method for [8-^2H]AMPPCP and $AMPPCD_2P$ as they were titrated with Mg^{2+} at both pH 7.0 and pH 10.0. Titrations were performed at concentrations of AMPPCP where self-association should be negligible (Tribolet & Sigel, 1988; Lam & Kotowycz, 1977). The pH 10 experiments were terminated at [Mg]:[AMPPCP] = 2.0, at which point $Mg(OH)_2$ began to form a precipitate. Chemical shift changes during titrations were negligible; 5–13 variable delay points were acquired, and delay versus intensity data were fit to a single-exponential equation by using a Bruker nonlinear fitting routine. The pulse repetition rate was in all cases $>5T_1$.

T_2 was determined from line widths when AK was titrated with $AMPPCD_2P$, $MgAMPPCD_2P$, [8-^2H]AMPPCP, and [8-^2H]AMP by using nucleotide concentrations of 0.5–15 mM. A single titration generally took 20–25 h, with no loss of AK activity and no hydrolysis of nucleotides as judged by silica gel TLC. Duplicate runs were performed in all cases. Spectra were acquired by using 90° pulses (12 μs), and pulse sequences CYCLOPS or RIDE (when acoustic ringing was observed to be a problem; Gerothanassis, 1987). The spectral resolution was 0.2–15 Hz/point (the higher values when very broad nucleotide peaks were observed) and was always more than sufficient to allow accurate definition of line shapes. The spectral width was always at least 10 times the line width of the broadest peak present. The repetition rates were greater than $5T_2$. In the case of studies at 77.8 MHz, an alternating phase pulse sequence was utilized and the FID was left-shifted following acquisition to reduce the effects of acoustic ringing. FIDs were zero-filled. The FID was further processed by exponential multiplication. Line widths $\Delta\nu_{1/2}$ were determined by using the Bruker program GLINFIT, which allows fitting of a peak to a Lorentzian function and calculation of the line width at half-maximal height for the fit. A Lorentzian line shape was observed in all cases. T_2 were determined from the simple relationship $\Delta\nu_{1/2} = 1/\pi T_2$.

The T_1 and T_2 of HDO present in all samples are much longer than that of deuterated AMPPCP partially bound to AK. Thus, while the dwell time during which the FID was sampled was sufficiently long to allow full decay of the AMPPCP component of the FID (whose T_1 and T_2 are <20 ms), the HDO component was truncated. This resulted in distortion of the "wings" of the HDO peaks. This was a serious problem since the HDO resonance is superimposed upon the much broader AMPPCP resonances. This problem was dealt with, when encountered, by further apodization. The FID was subjected to a cosine bell function. This artificially forced the tail of the FID (containing only the HDO component and noise) to zero while not affecting the early portion of the FID (containing all of the quickly decaying AMPPCP resonance) and thereby eliminated spectral distortion.

Proton NMR Methods. Binding studies were performed by titrating AK or peptide samples and taking the proton NMR spectrum at each point. All experiments were performed on a Bruker AM-500 spectrometer using an alternating phase pulse sequence with HDO peak suppression being accomplished by selective preirradiation. The spectral width was usually 6000 Hz with 16K or 32K data points, resulting in a spectral resolution of 0.3–0.8 Hz/point. The total pulse repetition rate was >3 s. Spectra were referenced either to external TSP or to the internal TSP peak for the *first* point in a titration. This was done because high concentrations of nucleotides induced concentration-dependent shifts in the reference peak, presumably due to nonspecific interactions between the nucleotides and TSP.

Viscosity Studies. An Ostwald viscometer was submerged (up to 1.5 cm from its top) in water contained in a 1-L graduated cylinder at room temperature (23 °C). Flow times were determined for various solutions in the viscometer, and densities were determined for the corresponding solutions by weighing them in a 2-mL pyncometer. Relative viscosities were calculated (using water as a reference) by using the equation (McKie & Brandts, 1972)

$$\text{relative viscosity} = (\text{density of solution} \times \text{flow time of solution})/(\text{density of water} \times \text{flow time of water}) \quad (6)$$

Because correlation times are usually viscosity dependent regardless of the type of associated motion (London, 1980; Boere & Kidd, 1982), we examined the possibility that our results could have been complicated by viscosity changes occurring during the course of the titrations. This concern is mainly for enzymic systems, which typically involved the titration of a 1–2 mM solution of AK with 75 mM nucleotide over a concentration range of 0–20 mM. To estimate the amount of viscosity change that could occur during such titrations, solutions of 1–2 mM chymotrypsin (27 kDa) and lysozyme (14 kDa) were titrated with 75 mM ATP from 0 to 20 mM, and the solution viscosities were measured (at pH 7 and 23 °C). These titrations allowed estimation of the change in viscosity of AK under conditions similar to those in our NMR titrations as lysozyme is somewhat smaller than AK (21.7 kDa) and chymotrypsin is somewhat larger. In both bases the total change in relative viscosity was <5% during the titrations. The viscosity change during the titration of AMPPCP with Mg^{2+} was estimated as <3% by analogous methods.

NMR Line-Shape Simulations. NMR line shapes for a simple two-site exchange system were simulated by use of a variant of the modified Bloch equation for two-site exchange (Sutherland, 1971). For a given set of parameters, intensities were calculated over a frequency range of at least 10 times the maximal possible calculated line width (i.e., 1000 Hz) with

resolution sufficient to adequately define the simulated spectral lines.

Proton NMR Titration Experiments and Binding Analysis. Complete titration experiments were carried out in all cases (by titrating the enzyme solution with the ligand and taking the 500-MHz ^{1}H NMR spectrum at each point), except AK–$MgAP_5A$ and AK–equilibrium mixture, where only one point with excess ligands (more than enough to saturate the enzyme) was taken. Typically 200–500 transients were taken for each point. The observed spectra were characteristic of fast exchange (or nearly so) and could therefore be used to monitor the concentration dependence of ligand–AK association. It should be noted that two of the four histidine C2–^{1}H peaks (peaks 3 and 4 in Figure 6) were insensitive to ligand binding but would be perturbed by significant variations in the pH (Tian et al., 1988). In the few instances where significant shifts in these peaks were observed, the histidine resonances (pH sensitive) were not used in the binding analysis. For individual peaks, plots of the free ligand concentration versus the observed chemical shift were fitted to 1:1 and, occasionally, 2:1 binding equations.

Binding of AMP and Adenosine from TLC Assays of the AK Reaction. We measured the K_i of AMP and adenosine as inhibitors of AK (competitive with MgATP) since elucidation of K_d from proton NMR was complicated by binding to the AMP site in the case of AMP and by limited solubility in the case of adenosine. Because high levels of either compound might also inhibit the coupling enzymes present in the standard spectrophotometric assay (Tian et al., 1988), we used a direct assay employing PEI–cellulose and radioactive ATP (Pederson & Catterall, 1979; Tomasselli & Noda, 1979). Detailed procedures have been described in Sanders (1988).

Synthesis and Separation of Isomers of $Cr^{III}(H_2O)_4ATP$. The screw-sense isomers of β,γ-bidentate $Cr^{III}(H_2O)_4ATP$ (CrATP) were synthesized and purified according to the procedures established previously (Dunaway-Mariano & Cleland, 1980a; Gruys et al., 1986). The products were separated by use of a C-18 reverse-phase preparative HPLC column (10 × 250 mm). The mobile phase was 0.01 M methanesulfonic acid, pH 2.5, at ambient temperature (25 °C), and the elution was followed with the absorbance at 256 nm. The four isomers were collected separately and cooled on ice. The isolated isomers were kept at 4 °C and were stable at this temperature as a dilute solution for about a week.

Since these isomers may undergo conformational isomerization ($1 \rightleftharpoons 4$ or $2 \rightleftharpoons 3$), epimerization ($1,4 \rightleftharpoons 2,3$), and hydrolysis (or dissociation), and these processes are very sensitive to pH, temperature, ionic strength, etc. (Gruys et al., 1986), it is important to address these properties under our experimental conditions. Although Gruys et al. (1986) reported that epimerization is negligible relative to conformational isomerization in the pH range 5.3–6.2 and that above pH 6.2 epimerization starts to occur at a significant rate, we observed that epimerization and conformational isomerization occurred at comparable rates in the pH range 5.8–6.1. The first-order rate constants of the disintegration of CrATP isomers, based on the decrease of the peak intensity, at pH 6.1 (70 mM MES buffer, 0.1 mM CrATP), 25 °C, were 0.017, 0.013, 0.008, and 0.010 min^{-1} for isomers 1, 2, 3, and 4, respectively. These values are in the range suitable for steady-state kinetics and for monitoring the epimerization by HPLC. Thus, we carried out all experiments in the pH range 5.8–6.1. Under such conditions the activity of AK was still at more than 50% of the optimal activity (k_{cat} = 420 s^{-1} compared with 670 s^{-1} at optimal pH).

Epimerization Reactions of CrATP Isomers. The CrATP sample obtained above was first concentrated in a rotary evaporator at 45 °C (within 45 min) and adjusted (with NaOH) to a pH (5.0) close to that of the reaction buffer (pH 5.8–6.1) but not high enough to induce epimerization. The nonenzymic reaction was initiated by adding the nucleotide sample to 75 mM MES buffer (containing 65 mM KCl, 1 mM DTE, pH 5.8–6.1 depending on specific experiments) to reach a final concentration of 0.1 mM. The exact pH value was then redetermined after mixing. At various time intervals, an aliquot (usually 20 μL) of the reaction mixture was withdrawn and injected into an analytical C-18 reversed-phase HPLC column (4.6 × 250 mm) preequilibrated with 0.01 M methanesulfonic acid, pH 2.5, at ambient temperature. For enzymic epimerization reactions, the enzyme was first dialyzed against the reaction buffer extensively and added to the reaction buffer to 0.6 mM. The reaction was again started by adding a certain volume of an isomer to the reaction buffer (containing the enzyme) to 0.1 mM and the final pH redetermnined. At different time intervals, an aliquot (100 μL) of the reaction mixture was withdrawn and mixed with 900 μL of the 0.01 M methanesulfonic acid elution buffer containing 90% ammonium sulfate. After vortexing for 1 min, the precipitated enzyme was removed by filtration through either a microfilter (ACRO LC13) or a glass pipet with a glass wool plug in the tip. The filtrate (50–100 μL) was then injected into the analytical column.

Inhibition of AK by CrATP. The steady-state kinetic studies were carried out by using the coupled enzyme method as described previously (Shyy et al., 1987) except that the reactions were carried out at 25 °C in the same MES buffer used in epimerization reactions. The enzyme was dialyzed against the MES buffer before use. The stock solutions of isomers of CrATP were preadjusted to ca. pH 5 and kept at 0 °C as described for epimerization experiments. To minimize epimerization and conformational isomerization, CrATP was added simultaneously with addition of the enzyme.

Results and Discussion

Determination of Relaxation Times and τ_c. Quadrupolar coupling constants (e^2qQ/h) for deuterated hydrocarbons are fairly invariant and change significantly only with major covalent changes in the vicinity of the C–D bond (Mantsch et al., 1977; Brevard & Kintzinger, 1978). Thus, in the metal ion titrations of deuterated AMPPCP, as well as in titrations of AK by AMPPCP, quadrupolar coupling constants can be assumed to be invariant during the course of the titrations. A value of 178 kHz can be utilized for [8–^{2}H]AMPPCP, which is the value determined for [8–^{2}H]AMP (Tsang et al., 1987) by solid-state NMR. For $AMPPCD_2P$ the value (168 kHz) determined for chemically analogous [$^2H_2$]malonic acid (Derbyshire et al., 1969) can be employed. The asymmetry parameter, η, is equal to 0 for axially symmetric electric field gradients and has a maximal value of 1 for maximal deviation from axial symmetry. As the C–D bond is axially symmetric, we assume $\eta = 0$. This assumption is supported by tabulations of experimentally determined values of η for deuterated hydrocarbons (Mantsch et al., 1977). These values, along with rigorous experiments and theoretical analysis, have allowed accurate determination of τ_c values of the phosphonate chain and the adenine ring of free and bound AMPPCP and AMP according to eq 1 and 2.

Table I lists the deuterium NMR relaxation times (T_1 or T_2) along with the effective correlation times τ_c. In terms of T_1 versus T_2, the latter is easier and was used in AK–nucleotide complexes where the line widths are broad enough to justify

Table I: Summary of Relaxation Times and Effective Correlation Times[a]

species	T_1 or T_2 (ms)	line width (Hz)	τ_c (ns)
free nucleotides			
AMPPCD$_2$P, pH 7.0	28 ± 3		0.084 ± 0.008
[8-^{2}H]AMPPCP, pH 7.0	15 ± 1		0.14 ± 0.02
AMPPCD$_2$P, pH 10.0	33 ± 2		0.072 ± 0.005
[8-^{2}H]AMPPCP, pH 10.0	15 ± 2		0.14 ± 0.02
Mg^{2+} complexes			
AMPPCD$_2$P, pH 7.0	14 ± 1		0.16 ± 0.02
[8-^{2}H]AMPPCP, pH 7.0	13 ± 2		0.16 ± 0.03
AMPPCD$_2$P, pH 10.0	16 ± 1		0.15 ± 0.02
[8-^{2}H]AMPPCP, pH 10.0	13 ± 2		0.16 ± 0.03
AK complexes (pH 7.0)[b,c]			
AMPPCD$_2$P	0.86 ± 0.01	370 ± 5 (345)	7 ± 1 (7.7 ± 2.1)
AMPPCD$_2$P + Mg^{2+}	0.48 ± 0.04	650 ± 50 (580)	15 ± 2 (14 ± 3)
[8-^{2}H]AMPPCP	0.25 ± 0.03	1280 ● 120 (1170)	28 ± 3 (26 ± 5)
[8-^{2}H]AMPPCP + Mg^{2+}	0.25	~1280[d]	~28
[8-^{2}H]AMP	0.26 ± 0.04	1240 ± 220	27 ± 5

[a] Obtained at 23 °C for free nucleotides and their complexes with Mg^{2+} and at 10 °C for all AK complexes. [b] The ratio [Mg^{2+}]/[AMPPCP] was maintained at 4.0 when Mg^{2+} is present. [c] Numbers in parentheses were repetitive experiments at 78.7 MHz; all other experiments were performed at 46.7 MHz. [d] This particular value was not obtained from a full titration experiment, but was assumed to be the same as for AK-[8-^{2}H]AMPPCP since addition of 0–2 equiv of Mg^{2+} to AK-[8-^{2}H]AMPPCP at fraction bound of 0.5 caused no detectable effect on the line width.

$\Delta\nu_{1/2} = 1/\pi T_2$. It is also important to note that in AK systems (around $\omega\tau_c = 1$) T_1 becomes rather insensitive to variation in τ_c. For free AMP and AMPPCP, and MgAMPPCP, T_1 were measured since in some cases line widths are narrow enough (10–25 Hz) that significant errors could be introduced by field inhomogeneity (2–3 Hz). Further details in the determination of T_1 and T_2 are described below.

While determination of the relaxation times of free nucleotides was straightforward, the relaxation times of the "bound species", i.e., MgAMPPCP and the various AK–nucleotide complexes, were obtained by titrating the nucleotide with Mg(II) or with AK, followed by data fitting. The titration data and curve fitting for AMPPCP/Mg(II), AMPPCP/AK, and AMP/AK are shown in Figures 1–3, respectively. This approach is different from previous studies involving the binding of ^{2}H-labeled ligands to proteins (Fenske & Cushley, 1984; Gerig & Hammond, 1984; Khaled et al., 1982; Viswanathan & Cushley, 1981; Neurohr et al., 1980; Zens et al., 1976; Oster et al., 1975; Glasel et al., 1973; Gerig & Rimerman, 1972), which have generally been based upon either direct observation of line widths from covalently or tightly bound species or the Swift–Connick equation (Swift & Connick, 1962; Luz & Meiboom, 1964) with the assumption of fast exchange conditions. Direct observation of the bound species cannot be achieved in AK–nucleotide complexes. The problem with use of the Swift–Connick equation is that the exchange rate should be determined accurately from an independent source and should be $\gg 1/T_{2,\text{bound}}$. Also, because only a small part of the fraction bound range is utilized in the Swift–Connick approach, extrapolation to the line width at fraction bound of 1 will necessarily contain a large uncertainty.

The plots of AMPPCP/Mg(II) in Figure 1 show a sharper increase before [Mg^{2+}]/[AMPPCP] = 1 and a slower increase

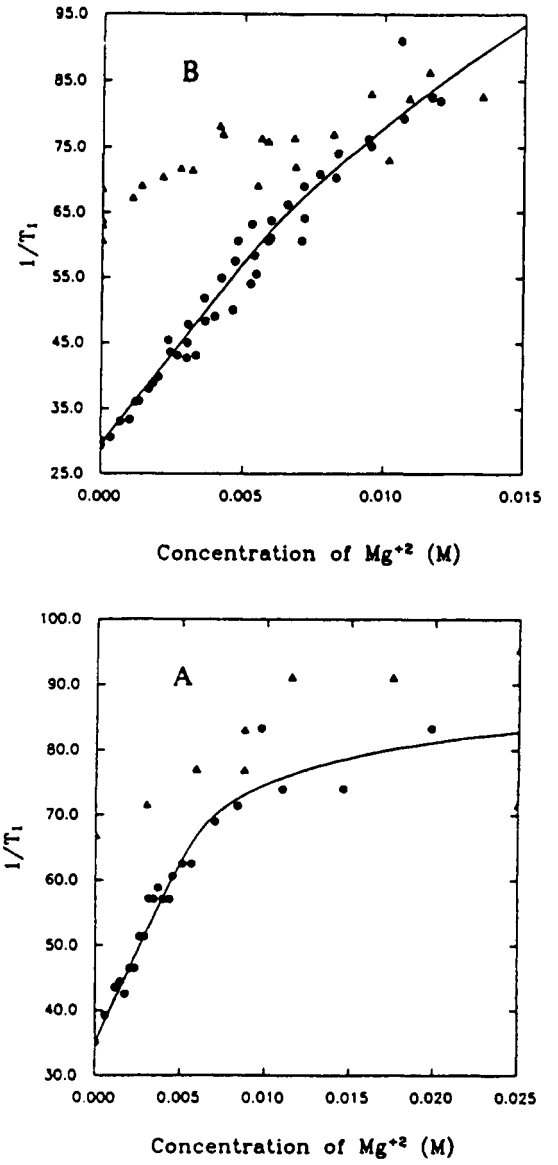

FIGURE 1: Variation of the ^{2}H NMR longitudinal relaxation rate at 23 ± 1 °C as a function of [Mg^{2+}]. Titrations were performed by adding $Mg(NO_3)_2$ to 6 mM solutions of AMPPCD$_2$P (●) and [8-^{2}H]AMPPCP (Δ) in 25 mM K^+Hepes, pH 7.0 (A), and in unbuffered H_2O, pH 10.0 (B). The data for AMPPCD$_2$P were fitted to a 2:1 binding model as described briefly in the text and in detail elsewhere (Sanders, 1988).

after the ratio exceeds 1, which is consistent with the 2:1 stoichiometry (tight/weak) previously observed qualitatively for AMPPCP (Vogel & Bridger, 1982) and quantitatively for ATP (Bishop et al., 1981; Mohan & Richnitz, 1974; Frey et al., 1972). The AMPPCD$_2$P data were fit to a 2:1 sequential binding model with $K_{d,1}$ held invariant at its independently determined values, 0.1 mM at pH 7, and 0.025 mM at pH 10 (Yount et al., 1971). Details of such data fitting are described in Sanders (1988). The T_1 values of MgAMPPCP listed in Table I were obtained from such fittings. It is important to note that the τ_c thus obtained for MgAMPPCD$_2$P is similar to that of MnATP (0.10 ± 0.01 ns) determined from the paramagnetic effects of Mn^{2+} on the T_1 of H_2O (Sloan & Mildvan, 1976). The data for [8-^{2}H]AMPPCP shown in Figure 1 are less quantitative due to shorter T_1 and smaller changes upon addition of Mg^{2+}. The T_1 values for [8-^{2}H]-AMPPCP listed in Table I were obtained from visual estimation of the data instead of curve fitting. Since the differences in T_1 values between free and Mg^{2+}-complexed [8-

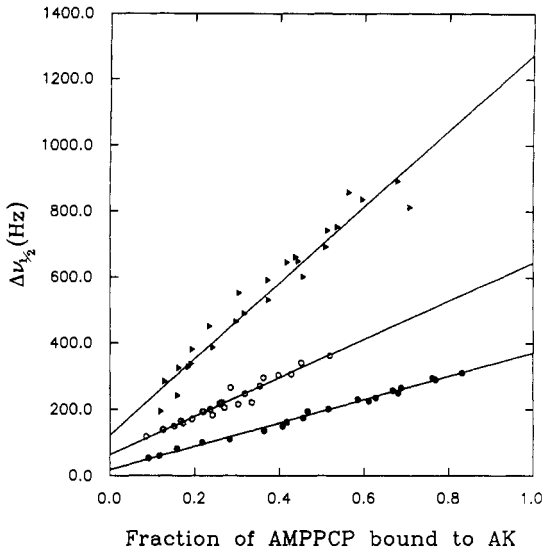

FIGURE 2: Variation of the 46.7-MHz ^{2}H NMR line widths ($\Delta\nu_{1/2}$) of AMPPCD$_2$P (●), MgAMPPCD$_2$P (○) (4:1 molar ratio of Mg^{2+} to AMPPCP), and [8-^{2}H]AMPPCP (▲) during titrations of AK at pH 7.0 and 10 °C by the nucleotide. Line widths have been corrected for the line broadening used in processing FIDs but have not been corrected for field inhomogeneity. Data fitting is described in Sanders (1988).

^{2}H]AMPPCP are small, possible errors from such estimation have little impact on the discussion and conclusion of this work.

The line widths of AK–nucleotide complexes listed in Table I were obtained from fitting of the titration data as follows. The data for AK complexes with AMPPCD$_2$P, [8-^{2}H]-AMPPCP, and MgAMPPCD$_2$P are presented in Figure 2 in a linearized form of a 1:1 binding model. The fits shown in the figure were performed while K_d was held at fixed values (0.22 mM for AMPPCP and 0.23 mM for MgAMPPCP) determined by ^{1}H NMR as described in a later section. Fits where K_d was also allowed to vary yielded dissociation constants that were within experimental errors of those determined independently by ^{1}H NMR. In the case of [8-^{2}H]AMP, ^{2}H NMR titration data (Figure 3) were fit to both 1:1 and 2:1 models with $K_{d,1}$ being fixed at 0.50 mM in the latter case (see proton NMR results). It was found that the 2:1 model gave a significantly better fit of the data than the 1:1 model (the sum of the deviations squared was half that of the 1:1 fit). The $K_{d,2}$ was calculated to be 7.9 ± 8.3 mM, which is only good enough to ascertain that the second binding is weak.

Although the measurement of relaxation times and the data fitting described above are accurate experimentally, the relaxation times of the bound species thus obtained represent true relaxation times only if the following assumptions are justified: (a) Line broadening due to ^{2}H–^{31}P or ^{2}H–^{14}N two-bond coupling does not contribute to the line widths when line widths were large and were used to determine T_2. The phosphonate methylene protons of AMPPCP couple with the neighboring phosphorus nuclei with a coupling constant of 21 Hz, while no coupling is observed between adenine nitrogens and the A-8 protons. Since ^{2}H–X coupling constants are approximately one-sixth of the corresponding ^{1}H–X constants (Mantsch et al., 1977), the effect of scalar coupling on line width is negligible. (b) The viscosity change during the course of the titration does not contribute to the observed line broadening. Our viscosity measurements as described under Materials and Methods suggested that the viscosity changes occurring during the ^{2}H NMR titrations were negligible. (c) The exchange rate is fast on the deuterium NMR time scale. This condition is easy to meet in the Mg(II)/AMPPCP system.

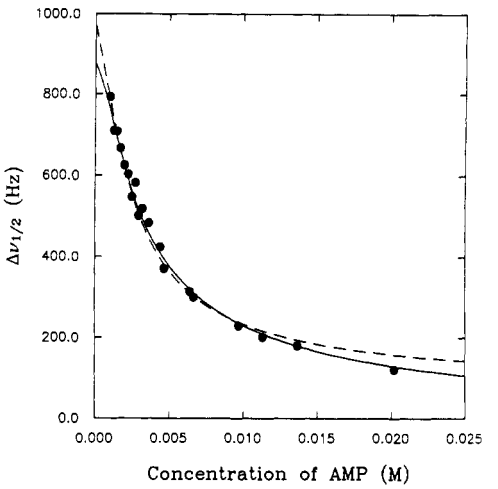

FIGURE 3: Variation of the 46.7-MHz ^{2}H NMR line width ($\Delta\nu_{1/2}$) of [8-^{2}H]AMP during titration of a 1.2 mM solution of AK with the nucleotide at pH 7.0 and 10 °C. Line widths have been corrected for postacquisition line broadening. The data have been fit to a 1:1 (dashed curve) and a 2:1 (solid curve) sequential AMP to AK binding models.

The exchange rate for Mg^{2+} on and off of ATP^{4-} is 1000–2000 s^{-1} (Vasavada et al., 1984) and is probably similar for $AMPPCP^{4-}$ present at pH 10 as the association constants of Mg^{2+} for ATP^{4-} and $AMPPCP^{4-}$ are similar (Yount et al., 1971; Dawson et al., 1986). This rate is likely to be even higher at pH 7.0, where AMPPCP possesses a charge of −3. The exchange rate greatly exceeds differences in chemical shift and relaxation rate differences between chelated and unchelated [8-^{2}H]AMPPCP and AMPPCD$_2$P. The observed relaxation rates are therefore "fast exchange" rates, which are the population-weighted average of chelated and unchelated AMPPCP (McLaughlin & Leigh, 1973). In the exchange systems involving AK, the justification of fast exchange is more complicated, and we have performed rigorous theoretical analysis and control experiments as described in the following section.

Validity of the Fast Exchange Approximation in AK–Substrate Systems. (a) Fast Exchange Relative to Chemical Shifts, i.e., $k_{ex} \gg (\nu_{bound} - \nu_{free})$.

$$1/k_{ex} = 1/(k_{on}AK_{total}) + 1/k_{off} \quad (7)$$

For our system shifts in frequency can be estimated from the ^{1}H NMR titrations. In our ^{1}H NMR titrations of AK, it was observed that the adenine C-8 proton of AMP, AMPPCP, and MgAMPPCP shifts less than 0.2 ppm upon binding to AK, while the methylene protons of AMPPCP and MgAMPPCP shift less than 0.1 and 0.6 ppm, respectively. This indicates that the maximal difference in frequency for the deuterium in free and bound nucleotides is only 28 Hz. As will be apparent in the following sections, the exchange rates for AMP, AMPPCP, and MgAMPPCP on an off of AK certainly exceed this value by well over an order of magnitude, and the condition of fast exchange with respect to chemical shift differences is easily met.

(b) Fast Exchange Relative to Relaxation Rates, i.e., $k_{ex} \gg (1/T_{2,bound} - 1/T_{2,free})$. In this case (when fast exchange with respect to chemical shifts also holds) a single Lorentzian peak will be observed. Even though Lorentzian line shapes were observed in all of our studies, extreme caution should be taken in presenting this as evidence for fast exchange. We have simulated spectra (see Materials and Methods) for the case where a bound species with line width of 1000 Hz is in exchange with free species with a line width of 20 Hz. Under

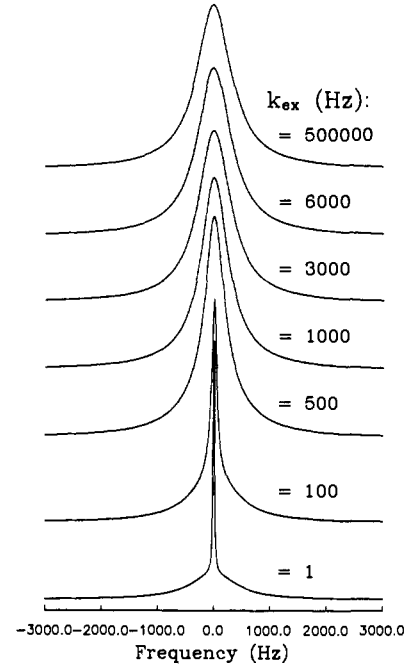

FIGURE 4: Simulated line shapes showing the effects of exchange upon the spectra of two exchanging species having the same intrinsic chemical shifts but differing in intrinsic relaxation rates. The broad species (relative population = 0.75) possesses an intrinsic line width of 1000 Hz, while the narrow species (relative population = 0.25) possesses an intrinsic line width of 20 Hz. Additional details of the simulations are found under Materials and Methods. The top five spectra are normalized in terms of total peak area with respect to each other, while the total area of the $k = 100$ and $k = 1$ spectra have total areas half and one-fourth those of the top five, respectively. In addition, close inspection will reveal that we have cut the top of the sharp component of the $k = 1$ spectrum short of its maximal value.

this condition $(1/T_{2,\text{bound}} - 1/T_{2,\text{free}}) = 3080$ Hz. It was assumed that there is no difference in the chemical shifts of bound and free species. The 75% bound case permits a good view of what happens as the exchange rate is varied from slow to fast conditions, as shown in Figure 4. At very slow exchange, the broad component and the sharp (free) component are both observed. However, even at the fairly slow rate of 500 Hz, the two components have become similar enough such that the noncomputational eye may not be able to discern that the peak is non-Lorentzian; indeed, at the signal-to-noise ratio at which quadrupolar NMR spectra are typically obtained, it may be impossible to discern by any method such deviations from Lorentzianality. This problem becomes even more pronounced at lower fractions bound where it may be difficult to observe the broad component, even in a very slow exchange situation.

Our confidence in the validity of the fast exchange approximation comes from the following theoretical analysis. The apparent line widths of the data shown in Figure 4 and additional simulations at different values of fraction bound were measured manually and plotted as a function of the fraction bound (Figure 5). Although fast exchange data (k_{ex} = 500000) yield a straight line as expected, the intermediate exchange data (k_{ex} = 6000 and 3000) are only slightly curved. This suggests that even if exchange is not fast, a fairly good estimate of the intrinsic line width of the fully bound species (fraction bound = 1) can be obtained provided a significant number of points are taken in the fraction bound >0.5 region. On the other hand, the curves in Figure 5 also suggest that the Swift–Connick approach, which extrapolates the initial portion of the curve to fraction bound of 1, could result in significant underestimation of the intrinsic line width of the

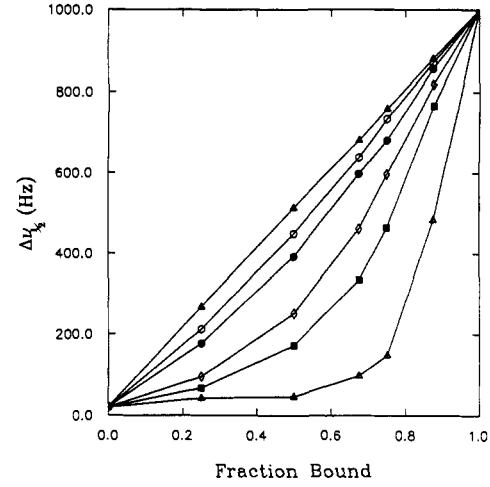

FIGURE 5: Simulated titration curves for 1:1 enzyme–ligand binding where the observed NMR line width ($\Delta\nu_{1/2}$) is complicated by chemical exchange. The apparent line width at half-maximal intensity is plotted against the fraction of the total ligand that is in the bound environment. The parameters used in spectral simulations are identical with those described in the caption of Figure 4 except that the relative populations were varied. The exchange rates k_{ex} for the curves are, from lower right, 100 (△), 500 (■), 1000 (◇), 3000 (●), 6000 (○), and 500000 (▲) Hz.

fully bound species if the fast exchange condition is not met rigorously. The linearity of the data for the three deuterated AMPPCP titrations beyond fraction bound of 0.5 (Figure 2) suggests that exchange of the nucleotides on and off of AK is effectively fast with respect to differences in relaxation rates of free and bound species.

(*c*) *Temperature Variation.* The simplest model for the relationship between τ_c and temperature is the Stokes–Einstein equation (Boere & Kidd, 1982)

$$\tau_c = 4\pi R^3\eta/3kT \qquad (8)$$

where R is the molecular radius, η is the absolute viscosity, k is Boltzmann's constant, and T is the absolute temperature. While this equation is derived for rigid, isotropic spheres, it does give one a feel for how temperature and viscosity should affect the data. Variable-temperature data were taken for $MgAMPPCD_2P$ and [8-^{2}H]AMPPCP (20 and 40% bound to AK, respectively), which in both cases display significant line narrowing as the temperature is raised. As described in detail in Sanders (1988), this result suggests that fast exchange approximation is justified in our systems.

(*d*) *Frequency Variation.* Equation 2 predicts that $1/T_2$ (and thus the line width) of bound species is frequency dependent, since the correlation times for the bound nucleotides are all well out of the extreme narrowing region (i.e., $\omega\tau_c \geq 1$). As shown in Table I, titrations at 78.7 MHz yielded correlation times (numbers in parentheses) that are in agreement, within experimental error, with those determined at 46.7 MHz. This justifies the fast exchange assumption and supports the suitability of the quadrupolar coupling constants utilized.

Structural Implications of the Motional Dynamics of AMPPCP. The correlation times determined reflect the rotational motion of the C–D bond axis (Huntress, 1970). They should be considered "effective" correlation times in that, for these molecules, τ_c is probably not determined by a single well-defined rotation but by a combination of overall AMPPCP tumbling and internal segmental motions. However, the overall correlation time establishes a lower limit to the timeframe of processes that will affect relaxation. Internal motions that are significantly (more than an order of mag-

nitude) slower than overall molecular tumbling will not influence relaxation behavior. The longest τ_c encountered in this study are 0.16 (for free AMPPCP) and 28 ns (for an AK bound species). Thus, our study can yield information on motions occurring at rates of approximately 10^8 and 10^6 s^{-1} and faster (for free and bound species, respectively; rates are based on the inverse of the correlation times minus 1 order of magnitude).

The τ_c for AK–AMPPCD$_2$P is significantly shorter than that of AK–[8-^{2}H]AMPPCP, suggesting that the phosphonate chain of the complex possesses considerable local mobility relative to the adenine ring at the active site of AK. The addition of Mg^{2+} to this complex reduces this local mobility substantially while not affecting that of the adenine ring. These results are reminiscent of the situation for AMPPCP free in solution.

The adenine ring appears to be totally immobilized upon binding of AMPPCP to AK. By use of the Stokes–Einstein equation, estimated viscosity, and the volume of AK determined by Pavlov and Fedorov (1983), the correlation time for AK at 10 °C is calculated to be 12 ns.[3] The τ_c of 28 ns determined for [8-^{2}H]AMPPCP is considerably longer. This is actually in accord with a number of studies (Anderson et al., 1970; Yguerabide et al., 1970; Hunkapiller et al., 1973; Cocco et al., 1978) that report the experimentally determined correlation times for proteins of approximately 20 kDa to be 15–30 ns: 2–3 times that predicted by the Stokes–Einstein equation. Work in Mildvan's laboratory (Fry et al., 1985; Mildvan & Fry, 1987) suggests that the adenine ring of MgATP bound to AK possesses a discrete conformation relative to the ribose, consistent with immobilization.

Assuming, therefore, that 28 ns represents the true overall τ_c for AK, the question arises as to whether the smaller τ_c for the phosphonate chain relative to the adenine ring of bound AMPPCP and MgAMPPCP result from internal motions which are of sufficient rate and amplitude to be significant in enzymic reactions. As noted earlier, internal motions must be on the order of, or faster than, the overall AK tumbling rate (i.e., $>10^6$ s^{-1}) to affect relaxation. The question of the amplitude of rotation can be inferred from London and Avitabile (1978), who examined the influence of the internal rotation of a methyl group upon the dipolar relaxation (mediated by C–H rotations) properties of the methyl ^{13}C. On the basis of their finding, and the consideration that dipolar and quadrupolar transverse relaxation mechanisms have similar dependences upon motion, it can be concluded that only rotations of the C–D bond vector of >40° and >80° amplitude could result in the differences in T_2 between AK–Mg[8-^{2}H]AMPPCP and AK–MgAMPPCD$_2$P and between AK–[8-^{2}H]AMPPCP and AK–AMPPCD$_2$P, respectively. These analyses suggest that the phosphonate chain does possess considerable local mobility relative to the adenine ring in both AK–AMPPCP and AK–MgAMPPCP.

The local mobility retained by the phosphonate chain could be accounted for by three possible effects. First, the hydrogen or ionic bonds may break and re-form many times during an AK–MgATP encounter. A similar phenomenon has recently been proposed for dihydrofolate reductase (Searle et al., 1988). It might also help account for (along with possible entropy effects) the observed binding energy of MgATP being only 6 kcal/mol, somewhat lower than might be expected in a binding situation where multiple highly specific (long lifetime) hydrogen bonds exist between counterions (Fersht et al., 1986; Bartlett & Marlowe, 1987). During the time where one or more of the hydrogen bonds is broken a portion of the phosphonate chain would be temporarily free to move around. The second possible explanation is that the intrinsic flexibility of the terminal amino groups of lysine and arginine side chains may allow the entire phosphonate–side chain complex to move around in a coordinated fashion (a sort of multiple tethering effect). Finally, the mobility could be explained on the basis of the *type* of energetics involved. The Debye–Huckel potential energy function for electrostatic interactions has an r^{-1} dependency (where r is the interionic distance), while the potential energy for dipole–dipole/van der Waals interactions (such as those expected between the adenine ring and hydrophobic or aromatic amino acids) has an r^{-6} dependency (Levine, 1983). The r^{-1} dependence of ionic interactions is spatially promiscuous, allowing favorable attraction to occur over a much wider range of distances for the dipole–dipole interactions. Thus, the phosphonate chain could move around a lot relative to the basic side chains of the binding site without compromising the energetics. This possibility is supported by affinity labeling studies (Yagami et al., 1988) in which adenosine di-, tri-, and tetraphosphopyridoxal all specifically label lysine 21. For the adenine ring any favorable dipole–dipole attraction with the hydrophobic cleft requires close, immobile interactions due to the r^{-6} dependency.

Previous ^{17}O NMR studies completed in our laboratory (Wisner et al., 1985) by using α-, β-, and γ-^{17}O-labeled ATP with AK suggest qualitatively that the terminal phosphate possesses more mobility than the β phosphate which, in turn, possesses more mobility than the α phosphate for the AK–ATP complex. Although use of ATP would be preferable to AMPPCP, deuterium NMR is much more quantitative than ^{17}O NMR since ^{17}O ($I = {}^5/_2$) has a large quadrupole moment and the relaxation behavior becomes multiexponential outside the extreme narrowing region (Forsen et al., 1987). While there are minor structural differences between ATP and AMPPCP, these differences do not appear to be significant for the purposes of this study. The p$K_{a,4}$ for ATP is approximately 7 (Ramirez & Marecek, 1980), while that for AMPPCP is ~8 (Vogel & Bridger, 1982; Schliselfeld et al., 1982), resulting in a net charge of ~−3.5 and ~−3 at pH 7 for ATP and AMPPCP, respectively. Complexation with Mg^{2+} lowers the p$K_{a,4}$ for both compounds such that at pH 7 both possess a net charge of −2 (see above references). AMPPCP and ATP exhibit very similar affinities for Mg^{2+} (Yount et al., 1971; Dawson et al., 1986) and are known to weakly complex a second Mg^{2+} (Vogel & Bridger, 1982; Bishop et al., 1981). Despite differences in the P–C–P and P–O–P bond angles, 117° and 130°, respectively, the P_β–P_γ distance for the two compounds remains nearly identical due to compensating bond length differences (Yount, 1975; DeLaMatter et al., 1973). Most importantly, we observed that AMPPCP and MgAMPPCP bind to AK at pH 7 at 10 °C with similar affinities to those of ATP and MgATP (see Table II).

Determination of Dissociation Constants and Local Binding Energy. Proton NMR was used as the main tool in determining the dissociation constant K_d of various substrates and analogues. The enzyme was titrated with the following substrates and analogues: AMPPCP, MgAMPPCP, AMP, ATP, MgATP, PPP_i, $MgPPP_i$, $MgPP_i$, adenosine, Mg^{2+}, and $MgAP_5A$. The proton NMR spectra of free AK and some of the complexes are shown in Figure 6, in which 15 easily observed individual peaks were labeled. The changes in δ of some or all of these peaks upon substrate binding have been

[3] This value is more accurate than the previous estimation of 75 ns (Sanders & Tsai, 1988).

Table II: Dissociation Constants and Binding Energies for AK–Ligand Complexes[a]

substrate/analogue	no. of titration points	range of concn (mM)	no. of K_d determined[b]	$K_{d,av}$ (mM)	$\Delta G°$ (kcal/mol)
MgAMPPCP	6	0–8	4	0.23 ± 0.13	−5.1 ± 0.4
AMPPCP	6	0–8	5	0.22 ± 0.10	−5.0 ± 0.5
MgATP	7	0–2.6[e]	6	0.17 ± 0.05	−5.2 ± 0.2
ATP	7	0–2.9[e]	6	0.044 ± 0.040	−6.3 ± 0.9
AMP (AMP site)	13	0–13	8	0.50 ± 0.25[c]	−4.6 ± 0.3
AMP (MgATP site)				4.3 ± 2[d]	−3.3 ± 0.3
Ado (MgATP site)	8	0–27	1	70 ± 30[f]	−1.6 ± 0.2
Ado (AMP site)				40 ± 20[f]	−1.9 ± 0.2
PPP_i	9	0–14	6	1.0 ± 0.4	−4.2 ± 0.4
$MgPPP_i$	11	0–19	6	1.7 ± 0.5	−3.8 ± 0.2
$MgPP_i$	6	0–6.9	5	5.5 ± 3	−3.1 ± 0.4
Mg^{2+}	7	0–560	0	>500	≈0

[a] Conditions were as described in the legend of Figure 6, except that MgAMPPCP and AMPPCP were determined at pH 7.0 and 10 °C in 6 mM Hepes buffer containing 65 mM KCl, 1 mM DTT, and 0.1 mM EDTA. [b] This is the number of K_d determined (for different resonances) that were used to actually calculate $K_{d,av}$. [c] This is the $K_{d,1}$ determined by combination of NMR and kinetic methods as described in the text. [d] This is the K_i of AMP inhibition against MgATP. [e] For both ATP and MgATP, points above 5 mM seemed to deviate from strict 1:1 behavior and were therefore not used in the calculation of dissociation constants. [f] The K_d determined by NMR for adenosine binding to AK was >30 mM. The values 70 and 30 mM were obtained from the K_i of adenosine inhibition against MgATP and AMP, respectively.

Table III: Changes in Chemical Shifts upon Ligand Binding to AK at pH 8.0 and 30 °C[a,b]

peak no.	δ_{free}	possible identity	change in chemical shift (ppm) upon binding by: AMP[c]	MgATP	ATP	ternary	$MgAp_5A$	$MgPPP_i$	PPP_i	$MgPP_i$
1	7.864	His-30	0.038	0.058	0.030	0.082	0.09	0.00	0.00	0.00
2	7.770	His-36	0.034	0.130	0.060	0.144	0.230	0.038	0.020	0.00
5	7.556		0.054	0.034	0.040	0.040	0.040	0.00	0.00	0.00
6	7.328		0.030	0.020	0.030	0.020	0.020	0.008	0.010	0.010
7	7.126		0.00	0.010	0.004	0.020	>0	0.004	0.00	0.00
9	6.958	His-30[d]	−0.010	−0.020	−0.020	−0.040	−0.040	−0.010	0.00	0.00
10	6.808		0.034	>0.0	0.038	?	?	0.024	0.034	0.018
11	6.454		0.020	0.040	0.014	0.060	0.066	0.00	0.00	0.00
12	6.330		0.038		0.036	0.100	0.090	−0.012	−0.008	0.010
13	6.294	Phe-12[d]	−0.220	?	−0.212	?	?	0.006	−0.080	0.010
14	2.056	Met	0.00	−0.020	0.00	−0.028	0.009	0.00	0.00	0.00
15	1.982	Met	0.008	−0.060	−0.032	−0.090	−0.100	−0.014	−0.018	−0.014
16	1.934	Met	−0.062	−0.044	−0.044	−0.046	−0.050	0.00	0.00	0.00
17	0.232		−0.02	−0.026	−0.03	−0.04	−0.04	−0.008	−0.006	−0.01
18	0.067		0.020	0.03	0.026	0.05	0.04	0.008	0.006	0.001

[a] See Figure 6 for peak labeling. The minus sign indicates an upfield shift. [b] Peaks 3, 4, and 8 did not undergo any significant shifts upon binding of any ligands. [c] The data for AMP were obtained from fitting to the 1:1 model. [d] Assignments of these are tentative.

monitored throughout the titration. In most cases data were fit to the 1:1 binding model with satisfactory results, and the dissociation constants thus determined are reported in Table II along with additional details of the individual titrations. Some representative titration curves are shown in Figure 7. The possible nature of these peaks and the $\Delta\delta_{max}$ values are listed in Table III. Since we found that AMP is a competitive inhibitor (with MgATP) of AK with a K_i of 4.3 mM, we fitted the data of AMP titration (up to 50 mM) to a 2:1 model with $K_{d,2}$ (binding to the MgATP site) fixed at 4.3 mM. The fitting was satisfactory and gave a $K_{d,1}$ of 0.5 mM, which is consistent with that determined from steady-state kinetics (0.37 mM). Titration of AK by $MgCl_2$ up to a concentration of 0.5 M induced few changes in the spectrum of AK. The peaks observed to shift showed a linear dependence on the metal ion concentration, suggesting that Mg^{2+} interacts with AK extremely weakly in the absence of nucleotide (K_d > 0.5 M). Further details of the fitting have been described in Sanders (1988).

The binding constants determined above were used to calculate binding energies, which are listed in Table II. The local binding energies were then calculated from eq 4–5 (and analogous relationships) and are listed in Table IV. It is worth noting that for MgATP–AK interaction the observed binding energies for the various parts of MgATP are approximately additive, indicative of a small "connectivity" term for ground-state binding.

Table IV: Local Binding Energies for Portions of MgAMPPCP and MgATP

segment	ΔG^i (kcal/mol)
adenosine	−1.4 ± 0.4
2′-OH	~0[a]
3′-OH	~0[a]
$MgPPP_i$	−3.6 ± 0.4
$MgPPCP_i$	−3.5 ± 0.7
PPP_i	−4.7 ± 0.1
$PPCP_i$	−3.4 ± 0.7
AMP (MgATP site)	−2.1 ± 0.6
$MgPP_i$	−1.9 ± 0.5
Mg^{2+}	~0

[a] On the basis of the observation that the K_m for Mg2′-dATP and Mg3′-dATP are approximately equal to that of MgATP.

Relationship of Local Substrate Dynamics to Local Binding Energy. Our results in Tables II and IV demonstrate that most of the binding energies that drive binding of ATP, MgATP, and MgAMPPCP derive from interactions of the triphosphate or triphosphonate moiety with AK. Adenosine supplies considerably less (with the 2′- and 3′-OH groups supplying none), and Mg^{2+} makes a negligible contribution. This is in complete accord with calculated interaction energies (Caldwell & Kollman, 1988) for the various segments of MgATP with AK using two of the existing binding site models and with previous binding/kinetic studies (Hiratsuka, 1983; Kappler et al., 1982; Hamada et al., 1979; Price et al., 1973). However, the deu-

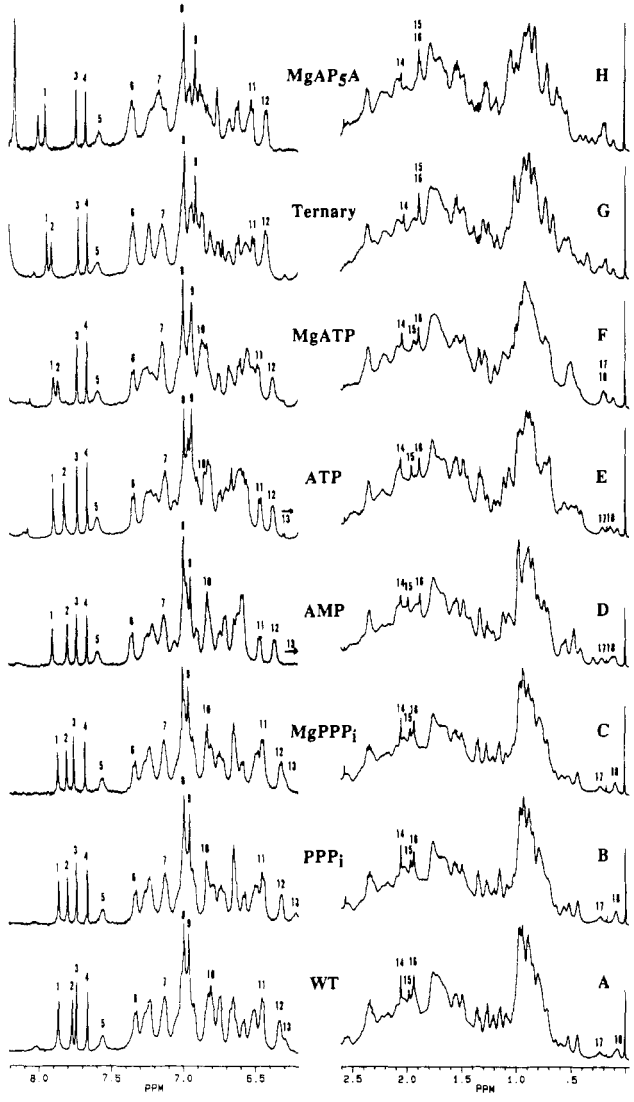

FIGURE 6: 500-MHz ^1H NMR spectra of native AK and its complexes with substrates and analogues at pH 8.0 and 30 °C after the FID was processed with 1 Hz of exponential line broadening: (A) 0.86 mM AK; (B) 0.4 mM AK + 7.8 mM PPP_i; (C) 0.25 mM AK + 19.4 mM PPP_i + 21.3 mM Mg^{2+}; (D) 0.74 mM AK + 4.5 mM AMP; (E) 0.5 mM AK + 9 mM ATP; (F) 0.4 mM AK + 8 mM ATP + 12 mM Mg^{2+}; (G) 0.37 mM AK + 9.3 mM AMP + 7.2 mM ATP + 10.7 mM Mg^{2+}; (H) 0.22 mM AK + 1 mM $MgAP_5A$. All solutions also contain 75 mM Tris-d_{11}, 65 mM KCl, 1.5 mM DTT, 1 mM K^+Hepes, and 0.1 mM EDTA. NMR procedures and sample preparation are described under Materials and Methods. It should be noted that in all titration experiments described in this paper (including ^1H and ^2H NMR) the Mg^{2+} to nucleotide ratios were kept at 4 at the early stage of titrations to minimize the existence of free nucleotide, but were lowered at the final stage of titration to avoid formation of Mg_2ATP and other nonspecific interactions involving Mg^{2+}. In the $MgAP_5A$ complex (H), the most downfield resonance arises from excess AP_5A. The resonance to the left of peak 1 was assigned to a C2H of bound AP_5A by Rösch et al. (1989), but our studies using site-specific mutants suggested it to be the C2H of His-36 (i.e., peak 2) (H. Yan and M.-D. Tsai, unpublished results).

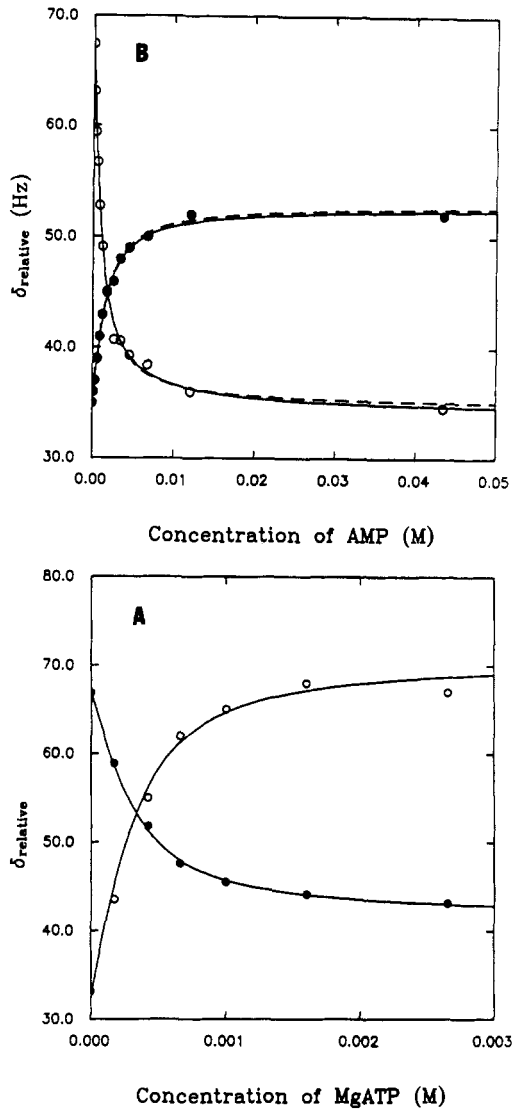

FIGURE 7: Examples of curves from titrations of AK by MgATP (A) and AMP (B) as followed by 500-MHz proton NMR at pH 8.0 and 30 °C. The open circles (○) and the solid circles (●) in (A) represent peaks 12 and 16, respectively, from Figure 6F, whereas the open and solid circles in (B) represent peaks 16 and 2, respectively, from Figure 6D. The data for AMP (B) were fitted to both 1:1 (dashed curves) and 2:1 (solid curves) models, while for MgATP (A) the curves shown are for 1:1 fits.

terium NMR results suggest that the adenine ring of both AMPPCP and MgAMPPCP is rigidly locked into place by AK, while the phosphonate chain of AMPPCP is fairly mobile at the MgATP site. Mg^{2+} reduces this local mobility considerably without significantly perturbing the thermodynamics of the system. On the basis of these observations *we conclude that there is no generalizable correlation between local binding energy and local mobility*. The observation of tight local binding energetically does not necessarily imply tight local binding motionally (and vice versa). Conversely, the observation of local mobility for one segment of a substrate cannot be taken to imply that the local binding energy for that portion of the substrate is weak (and vice versa).

Using a radioactivity assay system, we determined that $MgPPP_i$ as a substrate possesses a V_{max} 10^{-4}–10^{-5} times that of MgATP. Thus, the triphosphate moiety is a substrate by itself, but *the adenosine moiety is essential for optimal activity*. In addition, by use of 5′-deoxyadenosine and $MgPPP_i$ it was determined that optimal catalysis also requires the adenosine to be attached to the triphosphate, since 5′-deoxyadenosine did not enhance the activity appreciably as judged by using the radioactivity assay system. Thus, the adenine ring may play the role, mediated through the linking ribose, of an "anchor" for one end of the triphosphate chain. It is also interesting to note that there is a modest increase in the expression of binding energy for the adenine ring as it goes through the transition state as evidenced by the fact that $(V_{max}/K_m)_{MgATP}/(V_{max}/K_m)_{MgNTP}$ for AK and alternate nucleotide triphosphates are larger than the corresponding $K_{m,MgNTP}/K_{m,MgATP}$ (O'Sullivan & Noda, 1968). Thus, the

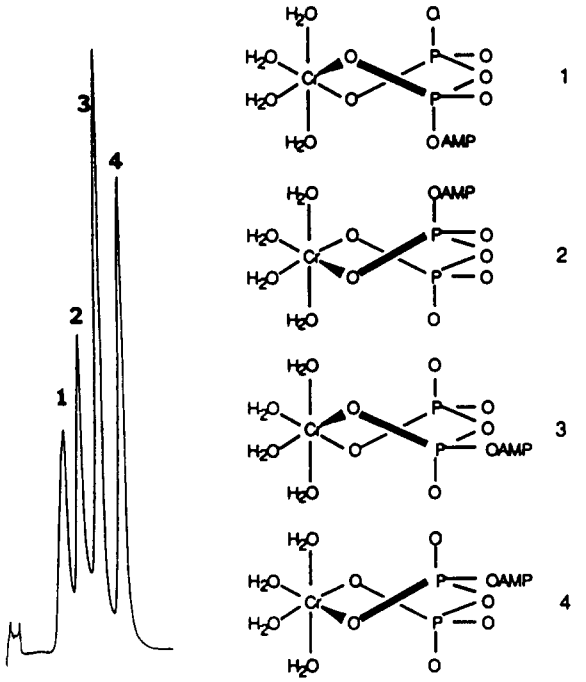

FIGURE 8: HPLC profile and structures for isomers 1–4 of $Cr^{III}(H_2O)_4ATP$.

adenine ring could provide specificity at the transition state.

Binding of the Δ and Λ Isomers of CrATP to AK. If the triphosphate moiety of MgATP is bound rigidly, it will imply that the enzyme exerts stringent stereochemical constraint even at the ground-state substrate binding. This would predict that AK can bind only one of the two isomers (Δ and Λ) of CrATP. On the other hand, the presence of local mobility in the triphosphate moiety of MgATP, as has been suggested by our deuterium NMR results, will predict that the enzyme can bind both isomers and that interconversion between the two isomers is possible. Thus, the local substrate dynamics could have implication on the (ground state) binding specificity of AK.

Although the "transition-state stereospecificity" of AK has been shown to be the Δ isomer of β,γ-bidentate metal–ATP on the basis of studies with CrATP (Dunaway-Mariano & Cleland, 1980b) and ATPβS (Kalbitzer et al., 1983), the "ground-state stereospecificity" mentioned above has been controversial. Kalbitzer et al. (1983) showed that (R_p)- but not (S_p)-[β-^{17}O]ATP caused a line broadening in the Mn(II) EPR spectrum of the AK–MnATP complex. This would suggest that the triphosphate binding region exhibits stringent stereochemical requirements even in the ground state, which is somewhat inconsistent with the conclusion of deuterium NMR studies that the phosphonate chain of bound AMPPCP and bound MgAMPPCP possesses considerable local mobility at the ground state. The Mn(II) EPR result of AK is also different from that of creatine kinase, which showed that the stereochemical requirement is fully expressed only in the transition-state analogue complex E–MnADPαS–nitrate–creatine, not in the ground-state complex E–MnADPαS (Reed et al., 1986). Since the K_i has been reported only for the mixture of stereoisomers of CrATP (Dunaway-Mariano & Cleland, 1980b), we conducted the measurement for pure screw-sense isomers.

We used the HPLC procedure (Gruys & Schuster, 1982; Cleland, 1986; Gruys et al., 1986) to separate the isomers 1–4 of CrATP (Figure 8), where 1 and 4 are conformational isomers of the Δ isomer and 2 and 3 are conformational isomers of the Λ isomer. Using the mixture of isomers 1–4 (mixed before kinetic studies), we first showed that CrATP is a

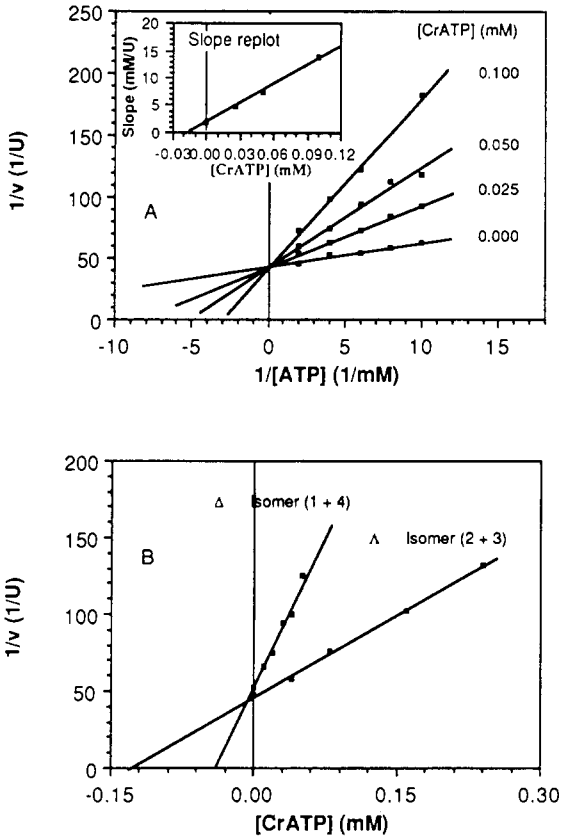

FIGURE 9: (A) Double-reciprocal plots showing the competitive inhibition of the reaction of AK by CrATP (mixture of all four isomers). The inset shows the slope replot. The K_i thus obtained is 16 μM. (B) Dixon plots of the inhibition of AK by CrATP:Δ isomer (1 + 4) and Λ isomer (2 + 3) at 0.250 mM MgATP. $K_i = K_m/(V_{max}[S] \times \text{slope})$ in the case of competitive inhibition. The K_i thus obtained are 11 and 20 μM for Δ isomer and Λ isomer, respectively.

competitive inhibitor against MgATP in the catalysis by AK (Figure 9A). Once this had been established, Dixon plots were used to determine K_i for separate isomers (Figure 9B). The K_i values thus obtained were 16, 11, and 20 μM for the mixture (isomers 1–4), the Δ isomer (1 + 4), and the Λ isomer (2 + 3), respectively. The K_m value of MgATP under the same condition was 43 μM. Although the K_i value may not necessarily be equal to the dissociation constant, the small difference between the two screw-sense isomers suggests that the binding affinity of AK for both isomers is very similar. This result, along with the observation that AK preferentially turns over the Δ isomer in the presence of AMP, suggests that AK expresses its full stereochemical specificity only at the transition state. The result is at variance with the observation of stereospecific interaction between the metal ion and the *pro-R* oxygen of the β-phosphate of ATP in the AK–MnATP complex (Kalbitzer et al., 1983). It should be noted that the same paper also reported lack of coordination between Mn(II) and the γ-phosphate of ATP, which also contradicts the results of recent NMR studies (Ray et al., 1988). The latter reported that the Co(II)–^{31}P distances of β-P and γ-P in AK–CoATP are in the range 3.1–3.5 Å, appropriate for first coordination sphere.

Effects on AK on the Epimerization of the Δ and Λ Isomers of CrATP. The ground-state stereospecificity also relates to a previously unaddressed question concerning the catalytic mechanism of AK. For those kinases with no stereochemical requirement at the ground state, the "wrong isomers" will bind as nonproductive complexes. In the case of AK, not only wrong stereoisomers but also wrong positional isomers may

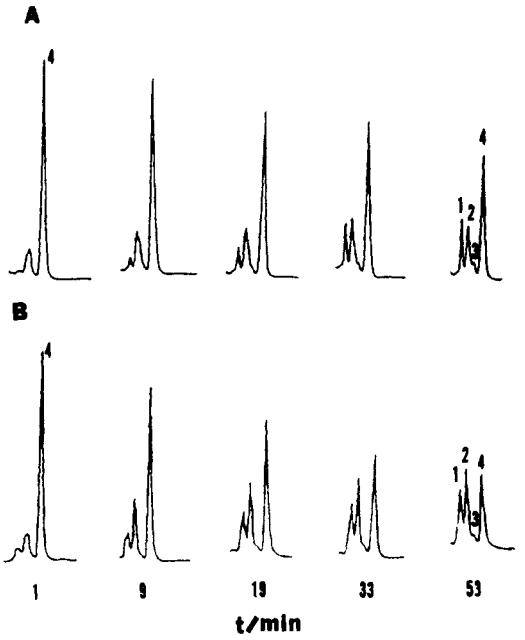

FIGURE 10: HPLC profiles showing the effect of AK on the epimerization and conformational isomerization of the isomer 4 of CrATP. The reaction condition was 0.1 mM CrATP 4 alone (A) and in the presence of AK (B) in 70 mM MES buffer, pH 5.9, 25 °C. The mobile phase was 0.01 M methanesulfonic acid. The flow rate was 1 mL/min and chart speed 1 mm/min.

bind to the enzyme, since the K_i of bidentate and tridentate CrATP are the same (11 μM, as mixtures of stereoisomers in both cases) (Dunaway-Mariano & Cleland, 1980b). This suggests that in the case of MgATP, which exists as an equilibrium mixture of predominantly bidentate and tridentate isomers (Huang & Tsai, 1982; Pecoraro et al., 1984), only ca. 20% of the mixture may exist in the correct mode (Δ, β, γ) and bind to AK productively. If the nonproductive AK–MgATP complexes can only dissociate, AK could only operate at ca. 20% of its catalytic capacity. Thus, it is important to ask *whether a nonproductive complex at the ground state can be converted to a productive complex without going through the process of dissociation and reassociation.*

In an effort to understand this problem, we investigated the effect of AK on the rate of epimerization between the Δ and the Λ isomers of CrATP. The epimerization of each isomer, 1–4, was monitored by HPLC in the absence and presence of AK. In the latter experiments, enough enzyme was used to allow binding of at least 90% of the nucleotide. Figure 10 shows the result of isomer 4. In Figure 10A (in the absence of AK) isomer 4 was converted to isomer 1 (conformational isomerization) and isomer 2 (epimerization). There was also a trace of isomer 3 formed. In the presence of AK (Figure 10B), similar processes occurred, except that epimerization was now slightly faster than conformational isomerization and small amounts of unidentified byproducts were formed.

Figure 11 shows the plots of the time course of epimerization for all isomers. Since we are only interested in the epimerization and there are insufficient data to determine quantitative rate constants for all processes (epimerization, conformational isomerization, and potential side reactions in the presence of AK), we plot the intensity ratios [1 + 4]/[2 + 3] as a function of time for isomers 2 and 3 and [2 + 3]/[1 + 4] for isomers 1 and 4.

The results demonstrate that all isomers of CrATP can undergo epimerization at the active site of AK. Epimerization appears to be faster in the presence of AK, and the "enhancement" was retarded by addition of ATP as shown in

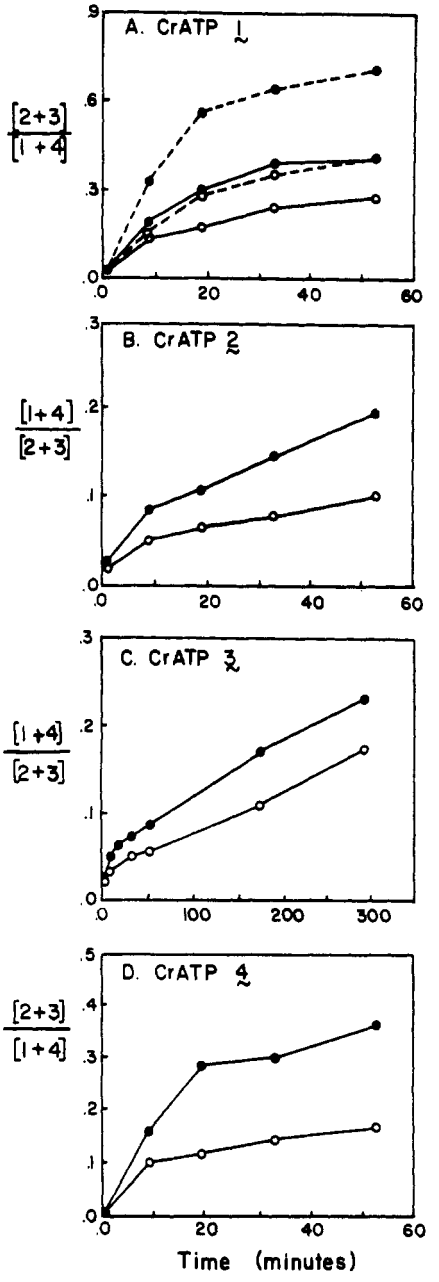

FIGURE 11: Plots of the time course of epimerization for CrATP isomer 1 (A), isomer 2 (B), isomer 3 (C), and isomer 4 (D), in the absence (○) and presence (●) of AK. In (A), the solid lines and the dashed lines were obtained at pH 5.9 and pH 6.0, respectively. (B) and (D) were obtained at pH 5.9, whereas the plots in (C) were obtained at pH 5.8. The ratios were calculated from the peak areas measured by enlarging, cutting, and weighing the paper. Possible errors in the measurement of peak areas are ±7%.

Figure 12A. However, it is doubtful whether the enhancement by AK can be regarded as significant. It is no more than a factor of 2 and could be at least partially due to unidentified side reactions. One the other hand, it may be argued that the 2-fold enhancement for CrATP, if real, could be much higher for MgATP due to lower energy barrier in the epimerization of MgATP. We therefore conclude that AK at least freely "allows" epimerization of CrATP (thus also MgATP). It may or may not catalyze the epimerization, but it definitely does not inhibit it. The same conclusions also apply to the process of conformational isomerization.

Since the Δ isomer is readily turned over by AK in the presence of AMP (Dunaway-Mariano & Cleland, 1980b), isomer 2 (Λ isomer) was used to examine the effect of AMP on the rate of epimerization. Plots of the decay of the peak

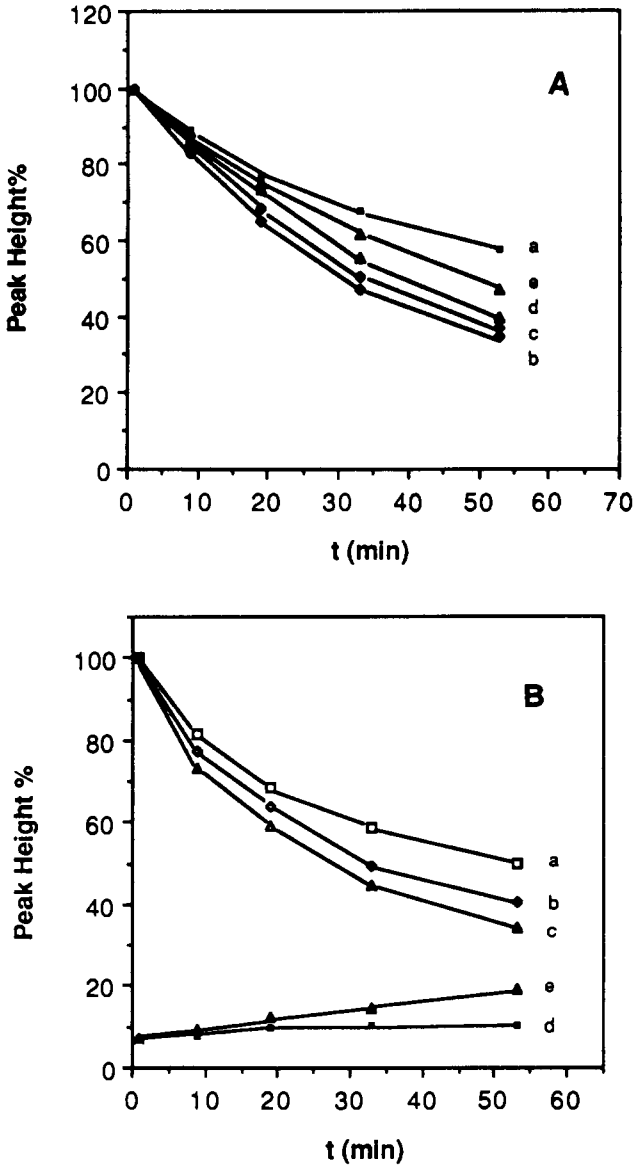

FIGURE 12: (A) Plots of the time course of the disintegration (on the basis of peak heights) of the isomer 4 of CrATP, showing the retardation of the AK-enhanced effect by ATP: (a) CrATP alone; (b) CrATP + AK; (c–e) same as (b), with 0.1, 0.2, and 0.4 mM ATP present. A control experiment showed no effect of ATP in the absence of AK. (B) Plots of the time course of the disintegration (on the basis of peak heights) of the reactions of the isomer 2 of CrATP, showing the effect of saturation of the AMP site of AK; (a) isomer 2 alone; (b) isomer 2 + AK; (c) isomer 2 + AK + AMP. Curves d and e represent the appearance of isomer 4 in (a) and (b), respectively. The reaction condition was 0.1 mM CrATP, 0.6 mM AK, and 2 mM AMP in 70 mM MES buffer, pH 6.0, 25 °C.

height of isomer 2 as shown in Figure 12B suggest that AMP does not affect the rate of epimerization. Again, the small enhancement in the presence of AMP may be insignificant and could be partially due to AK-catalyzed reaction between AMP and the Δ isomer of CrATP (formed from epimerization of the Λ isomer).

Relationship of Local Substrate Dynamics to Catalysis. Although the conditions used for the deuterium NMR and the CrATP studies were different due to practical limitations in experimental designs, our results suggest that the triphosphate site of AK is not stereochemically stringent in the ground state and allows epimerization and conformational isomerization between isomers of CrATP. This is fully consistent with the observation that despite the immobilization of the phosphonate moiety induced by Mg^{2+}, the ground-state AK–MgAMPPCP complex still possesses a certain amount of mobility in the β,γ-phosphonate region. The results also imply that in the case of MgATP the catalytically wrong screw-sense isomer, or even the wrong positional isomers, should also be able to "equilibrate" with the correct isomer while bound to the active site. This process allows the enzyme to "capture" different isomers of MgATP present in solution and utilize them with optimal catalytic efficiency. It is also reasonable that AK does not "catalyze" the process of epimerization, since there should be no evolutionary pressure to improve this process. Under standard assay conditions the k_{cat} of porcine muscle AK is 670 s^{-1}. The rate of exchange between MgATP and Mg(II) + ATP has been found to be 1.5×10^3 s^{-1} at 30 °C (Vasavada et al., 1984), 2×10^4 s^{-1} (Bryant, 1972), or 1.2×10^3 s^{-1} (Diebler et al., 1960). Since the rate of epimerization is an intramolecular process and should be much faster than the exchange rate, the epimerization between the Δ and Λ isomers of MgATP should be much faster than the turnover rate of AK. It should be noted that the situation is different in the case of substitution-inert CrATP. Under the conditions used (pH 5.8–6.1), the rate of epimerization should be slower than the turnover rate. Otherwise, both isomers should be equally good substrates for AK.

ACKNOWLEDGMENTS

We sincerely thank Dr. L.-Y. Hsu of The Ohio State University for writing the line-shape simulation program and for help in data plotting as well as S. Hakel for writing programs used in determining correlation times and for performing some of the viscosity studies. We are indebted to L. Brice for performing some kinetic studies, to J. Hart for purification of AK, to Dr. C. Cottrell for assistance in some NMR experiments, and to D. Weisenberger for obtaining the fast atom bombardment mass spectrum of tetraisopropyl [$^2H_2$]methylenediphosphonate.

REFERENCES

Abragam, A. (1961) *The Principle of Nuclear Magnetism*, Oxford University Press, London.

Allegrini, P. R., van Scharrenburg, G. J. M., Slotboom, A. J., de Hass, G. H., & Seeling, J. (1985) *Biochemistry 24*, 3268–3273.

Anderson, S. R., Brunori, M., & Weber, G. (1970) *Biochemistry 9*, 4723–4729.

Bartlett, P. A., & Marlowe, C. K. (1987) *Science 235*, 569–571.

Bishop, E. O., Kimber, S. J., Orchard, D., & Smith, B. E. (1981) *Biochim. Biophys. Acta 635*, 63–72.

Boere, R. T., & Kidd, R. G. (1982) *Annu. Rep. NMR Spectrosc. 13*, 320–385.

Brevard, C., & Kintzinger, J. P. (1978) in *NMR and the Periodic Table* (Harris, R. K., & Mann, B. E., Eds.) pp 107–128, Academic Press, New York.

Bryant, R. G. (1972) *J. Magn. Reson. 6*, 159–166.

Caldwell, J. A., & Kollman, P. A. (1988) *Enzyme 39*, 61–77.

Cleland, W. W. (1986) in *Mechanism of Enzymatic Reactions: Stereochemistry* (Frey, P. A., Ed.) pp 141–148, Elsevier, New York.

Cocco, L., Blakley, R. L., Walker, T. E., London, R. E., & Matwiyoff, N. A. (1978) *Biochemistry 17*, 4285–4290.

Dawson, R. M. C., Elliott, D. C., Elliott, W. H., & Jones, K. M. (1986) *Data for Biochemical Research*, 3rd ed., Clarendon Press, Oxford, U.K.

DeLaMatter, D., McCullough, J. J., & Calvo, C. (1973) *J. Phys. Chem. 77*, 1146–1148.

Derbyshire, W., Gorvin, T. C., & Warner, D. (1969) *Mol. Phys. 17*, 401–407.

Diebler, V. H., Eigen, M., & Hammes, G. G. (1960) *Z. Naturforsch. 15B*, 554–560.

Dunaway-Mariano, D., & Cleland, W. W. (1980a) *Biochemistry 19*, 1496–1505.

Dunaway-Mariano, D., & Cleland, W. W. (1980b) *Biochemistry 19*, 1506–1515.

Fenske, D. B., & Cushley, R. S. (1984) *Biochem. Biophys. Res. Commun. 121*, 871–877.

Fersht, A. R., Leatherbarrow, R. J., & Wells, T. N. C. (1986) *Trends Biochem. Sci. 11*, 321–325.

Forsen, S., Drakenberg, T., & Wennerström, H. (1987) *Q. Rev. Biophys. 19*, 83–114.

Frey, C. M., Banyasz, J. L., & Stuehr, J. E. (1972) *J. Am. Chem. Soc. 94*, 9198–9204.

Fry, D. C., Kuby, S. A., & Mildvan, A. S. (1985) *Biochemistry 24*, 4680–4694.

Gerig, J. T., & Rimerman, R. A. (1972) *J. Am. Chem. Soc. 94*, 7565–7569.

Gerig, J. T., & Hammond, S. J. (1984) *J. Am. Chem. Soc. 106*, 8244–8251.

Gerothanassis, I. P. (1987) *Prog. NMR Spectrosc. 19*, 267–329.

Glasel, J. A., Hruby, V. J., McKelvy, J. F., & Spatola, A. F. (1973) *J. Mol. Biol. 79*, 555–575.

Gruys, K. J., & Schuster, S. M. (1982) *Anal. Biochem. 125*, 66–73.

Gruys, K. J., Gregory, P. R., & Schuster, S. M. (1986) *J. Inorg. Biochem. 28*, 67–77.

Hamada, N., Palmieri, R. H., Russel, G. A., & Kuby, S. A. (1979) *Arch. Biochem. Biophys. 195*, 155–177.

Hiratsuka, T. (1983) *Biochim. Biophys. Acta 742*, 496–508.

Huang, S.-L., & Tsai, M.-D. (1982) *Biochemistry 21*, 951–959.

Hunkapiller, M. W., Smallcombe, S. H., Whitaker, D. R., & Richards, J. H. R. (1973) *Biochemistry 12*, 4732–4743.

Huntress, W. T. (1970) *Adv. Magn. Reson. 4*, 1–37.

Jencks, W. P. (1981) *Proc. Natl. Acad. Sci. U.S.A. 78*, 4046–4050.

Kalbitzer, H. R., Marquetant, R., Connolly, B. A. & Goody, R. S. (1983) *Eur. J. Biochem. 133*, 221–227.

Kappler, F., Hai, T. T., Abo, M., & Hampton, A. (1982) *J. Med. Chem. 25*, 1179–1184.

Khaled, M. A., Watkins, C. L., & Lacey, J. C. (1982) *Biochem. Biophys. Res. Commun. 106*, 1426–1434.

Kishi, F., Maruyama, M., Tanizawa, Y., & Nakazawa, A. (1986) *J. Biol. Chem. 261*, 2942–2945.

Lam, Y.-F., & Kotowycz, G. (1977) *Can. J. Chem. 55*, 3620–3630.

Levine, I. A. (1983) *Physical Chemistry*, 2nd ed., McGraw-Hill, New York.

London, R. E. (1980) in *Magnetic Resonance in Biology* (Cohen, J. S., Ed.) Vol. 1, pp 1–69, Wiley, New York.

London, R. E., & Avitabile, J. J. (1978) *J. Am. Chem. Soc. 100*, 7159–7165.

Luz, Z., & Meiboom, S. (1964) *J. Chem. Phys. 40*, 2686–2692.

Mantsch, H. H., Saito, H., & Smith, I. C. P. (1977) *Prog. NMR Spectrosc. 11*, 211–271.

McKie, J. E., & Brandts, J. F. (1972) *Methods Enzymol. 26*, 275–288.

McLaughlin, A. C., & Leigh, J. S., Jr. (1973) *J. Magn. Reson. 9*, 296–304.

Mildvan, A. S., & Fry, D. C. (1987) *Adv. Enzymol. Relat. Areas Mol. Biol. 59*, 241–313.

Moffatt, J. G., & Khorana, H. G. (1961) *J. Am. Chem. Soc. 83*, 649–658.

Mohan, M. S., & Richnitz, G. A. (1974) *Arch. Biochem. Biophys. 162*, 194–199.

Myers, C. T., Nakamura, K., & Danielzadeh, A. B. (1965) *J. Org. Chem. 30*, 1517–1520.

Neurohr, K. J., Lacelle, N., Mantsch, H. H., & Smith, I. C. P. (1980) *Biophys. J. 32*, 931–938.

Olah, G. A., & Nurang, S. C. (1982) *Tetrahedron 38*, 2225–2277.

Oster, O., Neireiter, G. W., Clouse, A. O., & Gurd, F. R. N. (1975) *J. Biol. Chem. 250*, 7990–7996.

O'Sullivan, W. J., & Noda, L. (1968) *J. Biol. Chem. 243*, 1424–1433.

Pavlov, M. Y., & Fedorov, B. A. (1983) *Biopolymers 22*, 1507–1522.

Pecoraro, V. L., Hermes, J. D., & Cleland, W. W. (1984) *Biochemistry 23*, 5262–5271.

Pederson, P. L., & Noda, L. (1979) *Methods Enzymol. 55*, 263–270.

Pharmacia P-L Biochemicals 1984 Product Reference Guide (1984) Pharmacia P-L Biochemicals, Piscataway, NJ.

Price, N. C., Reed, G. H., & Cohn, M. (1973) *Biochemistry 12*, 3322–3327.

Ramirez, F., & Maricek, J. F. (1980) *Biochim. Biophys. Acta 589*, 21–29.

Ray, B. D., Rösch, & Nageswara Rao, B. D. (1988) *Biochemistry 27*, 8669–8676.

Reed, G. H., Smithers, G. W., & Goodhart, P. J. (1986) in *Mechanism of Enzymatic Reactions: Stereochemistry* (Frey, P. A., Ed.) pp 177–187, Elsevier, New York.

Reynolds, M. A., Oppenheimer, N. J., & Kenyon, G. L. (1983) *J. Am. Chem. Soc. 105*, 6663–6667.

Rösch, P., Klaus, W., Auer, M., & Goody, R. S. (1989) *Biochemistry 28*, 4318–4325.

Roy, C. H. (1966) U.S. Patent 3 251 907; *Chem. Abstr. 65*, 3908d.

Sanders, C. R., II (1988) Examination of the Relationship of Substrate Dynamics to Enzymic Structure, Binding Energy, and Catalysis: NMR Studies of ATP and Adenylate Kinase, Ph.D. Dissertation, The Ohio State University.

Sanders, C. R., II, & Tsai, M.-D. (1988) *J. Am. Chem. Soc. 110*, 3323–3324.

Sanders, C. R., II, & Tsai, M.-D. (1989) *Methods Enzymol.* (in press).

Schenk, G. H., Hahn, R. B., & Hartkopf, A. V. (1977) *Quantitative Analytical Chemistry*, Allyn and Bacon, Boston.

Schliselfeld, L. H., Burt, C. T., & Labotka, R. J. (1982) *Biochemistry 21*, 317–320.

Schulz, G. E., Schiltz, E., Tomasselli, A. G., Frank, R., Brune, M., Wittinghofer, A., & Schirmer, R. H. (1986) *Eur. J. Biochem. 161*, 127–132.

Searle, M. S., Forster, M. J., Birdsall, B., Roberts, G. C. K., Feeney, J., Cheung, H. T. A., Kompis, I., & Geddes, A. J. (1988) *Proc. Natl. Acad. Sci. U.S.A. 85*, 3787–3791.

Shyy, Y.-J., Tian, G., & Tsai, M.-D. (1987) *Biochemistry 26*, 6411–6415.

Sloan, D. L., & Mildvan, A. S. (1976) *J. Biol. Chem. 251*, 2412.

Sutherland, I. O. (1971) *Annu. Rep. NMR Spectrosc. 2*, 71–235.

Swift, T. J., & Connick, R. E. (1962) *J. Chem. Phys. 37*, 307–320.
Tanizawa, Y., Kishi, F., Kaneko, T., & Nakazawa, A. (1987) *J. Biochem. 101*, 1289–1296.
Tian, G., Sanders, C. R., II, Kishi, F., Nakazawa, A., & Tsai, M.-D. (1988) *Biochemistry 27*, 5544–5552.
Tomasselli, A. G., & Noda, L. (1979) *Eur. J. Biochem. 93*, 262–270.
Tribolet, R., & Sigel, H. (1988) *Eur. J. Biochem. 170*, 617–626.
Tsang, P., Vold, R. R., & Vold, R. L. (1987) *J. Magn. Reson. 71*, 276–282.
Vasavada, K. V., Ray, B. D., & Nageswara Rao, B. D. N. (1984) *J. Inorg. Biochem. 21*, 323–335.
Viswanathan, T. S., & Cushley, R. J. (1981) *J. Biol. Chem. 256*, 7155–7160.
Vogel, H. J., & Bridger, W. A. (1982) *Biochemistry 21*, 394–401.
Wisner, D. A., Steginsky, C. A., Shyy, Y.-J., & Tsai, M.-D. (1985) *J. Am. Chem. Soc. 107*, 2814–2815.
Yagami, T., Tagaya, M., & Fukui, T. (1988) *FEBS Lett. 229*, 261–264.
Yguerabide, J., Epstein, H. F., & Stryer, L. (1970) *J. Mol. Biol. 51*, 573–590.
Yount, R. G. (1975) *Adv. Enzymol. Relat. Areas Mol. Biol. 43*, 1–52.
Yount, R. G., Babcock, D., Ballantyne, W., & Ojala, D. (1971) *Biochemistry 10*, 2484–2489.
Zens, A. P., Fogle, P. T., Bryson, T. A., Dunlap, R. B., Fisher, R. R., & Ellis, P. D. (1976) *J. Am. Chem. Soc. 98*, 3760–3764.

Human Deoxycytidine Kinase: Kinetic Mechanism and End Product Regulation†

Min-Young Kim and David H. Ives*
Department of Biochemistry, The Ohio State University, 484 West 12th Avenue, Columbus, Ohio 43210
Received March 29, 1989; Revised Manuscript Received July 3, 1989

ABSTRACT: The kinetic properties of the monomeric deoxycytidine kinase (EC 2.7.1.74) from leukemic human T-lymphoblasts have been investigated. The results of steady-state initial-rate kinetic analysis and product inhibition studies at pH 7.5 and 37 °C indicate that substrate binding follows an ordered sequential pathway, with the magnesium salt of ATP being the first substrate to bind and dCMP the last product to dissociate. At subsaturating substrate concentrations, dCMP produced competitve inhibition against ATP, while against varied deoxycytidine concentrations dCMP exhibited mixed-type inhibition. ADP produced noncompetitive inhibition against either substrate. The limiting K_m values for deoxycytidine and MgATP were 0.94 and 30 μM, respectively. The end product inhibitor dCTP exhibited competitive inhibition against varied ATP concentration, with a dissociation constant estimated to be 0.7 μM when extrapolated to zero ATP concentration. dCTP was purely noncompetitive against varied deoxycytidine concentration. On the basis of these kinetic results, and on the strong and specific inhibition by dCTP, it is proposed that this end product functions as a multisubstrate analogue, with its triphosphate group binding to the phosphate donor site of the enzyme and its deoxycytidine moiety overlapping and binding to the deoxynucleoside site in a highly specific manner.

Recent work in this laboratory has suggested a simple but very effective nonallosteric mechanism by which accumulating deoxynucleoside triphosphate end products may regulate at least some deoxynucleoside kinases in bacteria (Ikeda et al., 1986). It was found that these triphosphates behave kinetically very much like synthetic bisubstrate analogues in which are joined the 5′-hydroxyl of the deoxynucleoside, and of the adenosine moiety of ATP by tetrapolyphosphate. It was postulated that the nucleoside moiety of the end product deoxynucleotide binds, with great specificity, to the deoxynucleoside binding site on the enzyme and its phosphates overlap and bind to the ATP subsite. This combination of binding forces causes the triphosphate to be bound more tightly than either substrate.

Such a mechanism is possible only when substrate binding leads to formation of a ternary complex; i.e., both subsites must exist at the same time. However, the pattern of inhibition by end product, acting as a bisubstrate analogue, would depend on whether the kinetic mechanism were a random or an ordered sequential process (Fromm, 1977). This inhibitor should compete with both substrates in cases of random substrate binding, but only with the leading substrate in an ordered mechanism. Unfortunately, the kinetic mechanisms have been worked out for very few mammalian deoxynucleoside kinases. This can be explained, in part at least, by the nonlinear kinetic patterns observed in a number of instances. Mammalian cytosol thymidine kinase (EC 2.7.1.21) fractions have exhibited the sigmoidal ATP saturation curves and end product modulation characterisitic of cooperative binding in heterotropically regulated allosteric enzymes, although there is no direct proof of a regulatory site (Lee & Cheng, 1976; Munch-Petersen & Tyrsted, 1985). While classical cooperative behavior has not been observed with cytosol deoxycytidine kinase, both calf thymus (Ives & Durham, 1970; Kozai et al., 1972) and human deoxycytidine kinase preparations (Hershfield et al., 1982; Sarup & Fridland, 1987; Bohman & Eriksson, 1988) have yielded bimodal double-reciprocal plots. Kozai et al. (1972)

† This work was supported in part by Grant DMB-8416134 from the National Science Foundation and Grant OCRA-88-02-05 from the Ohio Cancer Research Associates. We also acknowledge the support of NIH Research Grant 2P30CA16058 from the National Cancer Institute.

0006-2960/89/0428-9043$01.50/0